Reservoir quality prediction of deep-water Oligocene sandstones from the west Niger Delta by integrated petrological, petrophysical and basin modelling

O.K. Chudi*, Helen Lewis, D.A.V. Stow, J.O. Buckman
Institute of Petroleum Engineering, Heriot-Watt University, EH14 4AS, Edinburgh, UK
Corresponding author-obinna.chudi@pet.hw.ac.uk,

Deepwater reservoir quality prediction

ABSTRACT: Petroleum exploration and production in the Niger Delta region to date has mainly focussed on the onshore, deltaic and offshore deep-water Miocene successions. Although Miocene turbidites have been the principal deep-water target to date, deeper-lying Oligocene sandstones are now being considered for exploration. This study targets an area beneath the Niger basin slope at a present-day water depth of 800-1500 m. Within this study area, the Miocene to Recent sands above a burial depth of 3600 m show very good reservoir quality with porosities as high as 35% and permeabilities in the Darcy range. The aim of this study is to predict the reservoir quality and properties of the Oligocene sandstones below 3800 m, using basin modelling to predict conditions where quartz cementation will take place and quartz cementation models to predict the amount of cementation and hence potential porosity loss. Modelling results show that the Oligocene sandstones have been exposed to conditions favourable for quartz precipitation, but that less than 14% of the original porosity will have been occluded by quartz cement. These results are in agreement with both elemental analysis from petrophysical and petrological observation of thin-sections. Although the deeper-lying Oligocene sandstones are likely to have reduced reservoir quality caused by the presence of quartz overgrowth cementation, it appears likely that the volume of cement is relatively low and that the Oligocene succession should be considered a viable play.

The Miocene clastic succession of the prolific Niger Delta province has since the 1950's been the major target for hydrocarbon exploration and is responsible for hosting most of the discoveries in both onshore and offshore parts of the delta system (Doust & Omatsola, 1990, Saugy & Eyer, 2003, Reijers, 2011). In part, this is due to the excellent porosity and permeability characteristics of the poorly consolidated reservoir sands (Weber, 1971). Porosities of up to 35% and permeabilities of more than 3 Darcy's have been reported from well logs and cores across producing fields in the delta region. There has been none to minimal cementation and very little precipitation of authigenic minerals, dominated by quartz overgrowths, within the primary porosity. Reservoir quality of the Miocene interval has been very little degraded.

As the quest for more hydrocarbon reserves increases, exploration and production is gradually moving from the shallow-burial and more easily identifiable reservoirs of the Miocene to deeper-lying Oligocene plays that have been exposed to higher temperatures and hence physical and chemical conditions more conducive to quartz precipitation. The aim of this study is to estimate the degree of quartz cementation of unexplored, deeply buried, Oligocene deep-water clastic sediments of the Niger Delta basin-slope region. We apply an integration and cross-comparison of basin modelling, cementation modelling, petrological analysis and petrophysical multi–mineral elemental analysis.

The Niger Delta has been the centre of attraction for hydrocarbon exploration and production on the continental margin of West Africa for over four decades (Haack et al., 2000) and consequently has been thoroughly studied (Short & Stauble, 1967, Weber, 1971, Whiteman, 1982, Ejedawe et al., 1984, Damuth, 1994, Haack et al., 2000). The delta is situated in the Gulf of Guinea and covers an area of approximately 140,000km^2 with a maximum clastic

sediment thickness of about 12km at the basin centre (Damuth, 1994). The study area is located in the translational tectonic province in the mid-slope of the Niger Delta deep-water system (Fig.1). The proven reservoir intervals are Miocene channel sands with porosity values greater than 30% and permeability in the Darcy range. Of over 30 wells drilled in the study area only one well penetrated the top of the Oligocene succession, which is the primary interval of interest to this study.
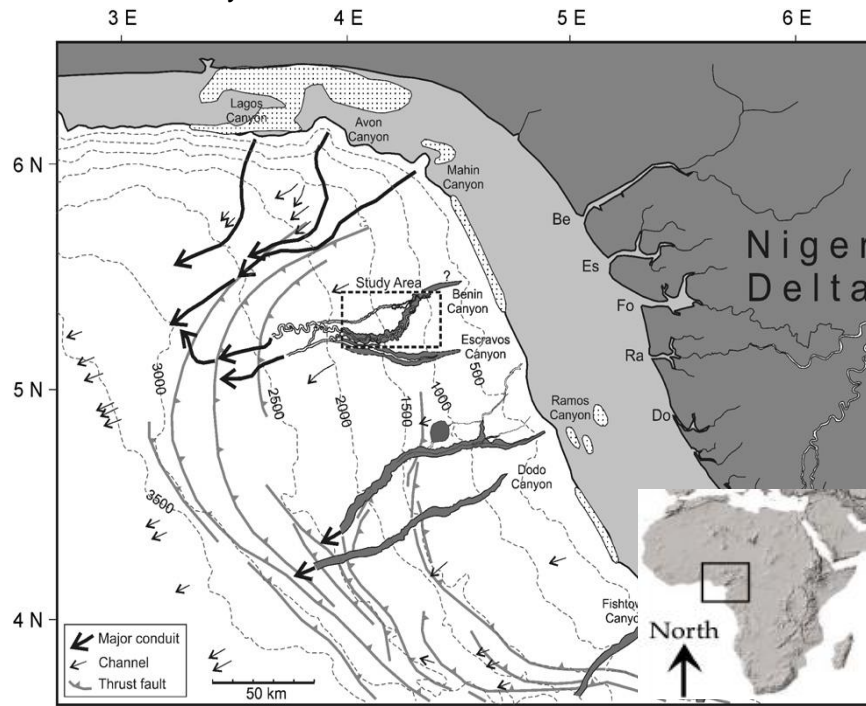

Fig. 1. Regional location map showing the western Niger Delta and study area (adapted from Deptuck et al., 2007).

Generally reservoir rock quality is controlled by variables such as the grain size, initial depositional porosity, mechanical compaction, chemical compaction, mineralogy and volume of pore filling cement (Worden & Morad, 2000). The diagenetic changes that influence reservoir properties, such as porosity and permeability, are affected by an interplay of these factors under conditions of increased effective stress, temperature and burial (Taylor et al., 2010). The regional geothermal gradient of the whole Delta region ranges from 1.3 to 1.8° C/100m in the centre of the basin and increases up-dip and northward to about 2.7 to 5.5° C/100m (Nwachukwu, 1976, Doust & Omatsola, 1990). These controlling variables have particularly influenced the strategy and the technique adopted herein for petrophysical evaluation across fields within the delta system.

The accurate prediction of sandstone reservoir quality is a key challenge for hydrocarbon exploration and production. A good understanding of reservoir quality is required throughout the entire life cycle of a reservoir; from exploration where it is required for initial hydrocarbon reserves estimation, to appraisal and development stages where porosity and permeability distribution in a reservoir are requisite for well placement optimization and to estimate economic cut-off limits that control estimates of hydrocarbon pore volumes, recoverable reserves and production rates (Sneider, 1990). A fundamental control of sandstone reservoir quality, especially for siliciclastic systems, is quartz cementation. This is controlled by

temperature, pressure (effective stress) and surface area of the quartz substrate, which is itself a function of grain size, abundance of grain coatings and quartz clast abundance (Walderhaug, 2000, Worden & Morad, 2000).

We present a synthesis of petrological, petrophysical and basin modelling studies in order to characterise the poorly understood potential Oligocene reservoirs of the mid-slope, deep-water part of the Niger Delta Basin. The focus of this work is to better understand and investigate the reservoir potential of the Oligocene interval buried below 3800m, most importantly its diagenetic history, using a novel integrated methodology. The burial, temperature and pressure histories have been considered, particularly their key controls on quartz cementation. Petrological analysis of thin sections and polished block samples of the hydrocarbon-charged shallower Miocene samples were studied and inferences made to predict the mineralogy of the uncored Oligocene interval that was penetrated by a single well (A1). The petrological study was integrated into multi-mineral petrophysical study to predict sandstone composition from well log responses. We further consider the applicability of this approach and these findings to analogous subsurface systems around the world.

GEOLOGICAL SETTING

Rifting and break-up of Africa from South America in this region initiated in the early Cretaceous, with a triple junction located approximately beneath the region that is now the Niger Delta. By the late Cretaceous, spreading of the Atlantic was underway along the southern and western arms of this tri-rift systems, whereas the north-eastern arm, the Benue Trough, became a failed rift system. Certainly by Palaeocene time, the Niger Delta region had begun to receive significant input of sediment from the land. Through the Palaeocene and Eocene, there were probably at least three principle depocentres linked to marked sediment progradation over the subsiding continental–oceanic lithospheric transition zone. By Oligocene time, these three depocentres had merged into the single major arcuate depocentre that is now the Niger Delta. Increased sediment load on a cooling and subsiding basement further enhanced subsidence in the region. Since this time the delta has prograded in a generally south–west direction creating a series of major depositional belts that represent the most active portion of the delta at each stage of development. The principal sediment provenance for the western delta region has been the Benue–Niger drainage system whereas the eastern delta region was sourced from the Cross River system. The present day Niger Delta complex takes the form of a constructive arcuate delta, with mud diapirism beneath the slope playing a major role in controlling sediment distribution (Whiteman, 1982).

Lithostratigraphy
The Tertiary Niger Delta complex comprises a tripartite lithostratigraphic sequence – the Benin, Agbada and Akata Formations (Fig. 2). Each of these Formations represents deposition in one of three main sedimentary environments: continental, transitional and marine, respectively. These depositional environments are arranged laterally from proximal to distal and, as a result of marked progradation, they also stack up vertically with the continental Benin Formation overlying the transitional (marginal marine) Agbada Formation, which in turn overlies the marine/deep marine Akata Formation. We describe each briefly below from proximal to distal.
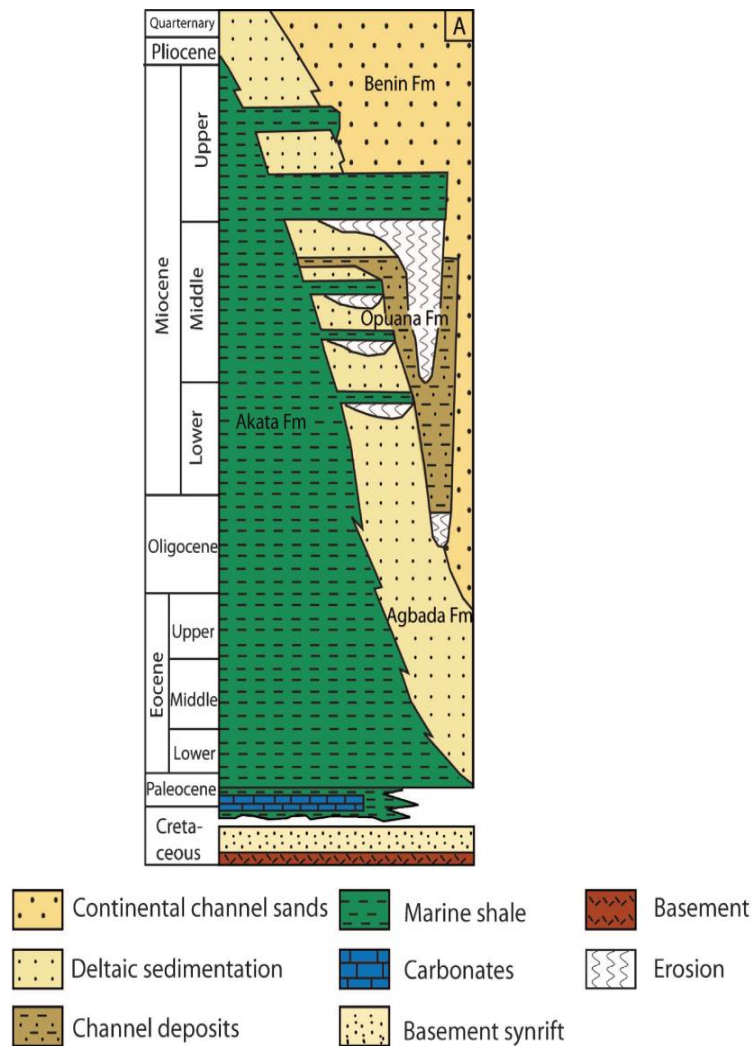
Fig. 2. Stratigraphy of the Niger Delta (after Corredor et al., 2005).

The proximal continental environments comprise sediments of the upper delta plain and fluvial feeder system and are represented by predominantly sandy lithologies. The sediments are poorly sorted, granular and pebbly, coarse to very fine grained. They are assigned to the Benin Formation that occurs wholly onshore at the present day, but which also extends a short distance offshore in the subsurface (Short & Stauble, 1967). The known age of the Benin Formation is from Oligocene to Recent although, presumably, an equivalent lithostratigraphic unit also acted as sediment source for the older delta deposits. The Benin Formation generally exhibits poor reservoir quality and so is not an effective reservoir target.

The transitional, marginal marine environment comprises interbedded sandstones and shales assigned to the Agbada Formation. The shale units are more prominent with depth becoming progressively thicker than the intercalated sandstone units; this reflects the seaward advance of the delta system through time (Whiteman, 1982). The sandstones constitute the principle reservoir units in the Niger Delta Basin, exhibiting excellent reservoir quality. They were most likely charged through large-scale open growth faults connected to adjacent kitchen areas. The Agbada Formation extends throughout the Niger Delta region and represents deposition in both lower delta plain and marginal marine to continental shelf environments.

The interplay between subsidence and sediment supply, and the relative change in sea level, has driven transgressive and regressive cycles responsible for alternating sandstones and shale sequences (Doust & Omatsola, 1990). The known age of the Agbada Formation ranges from Eocene to Recent.

The distal and fully marine environments are represented by a more mud-rich succession known as the Akata Formation. The marine shales of this sequence range from Palaeocene to Recent in age, and are mainly characterised by hemipelagic slope sediments intercalated with turbidite sandstones. Regional studies and experimental analysis suggest that the Akata Formation provides the principal hydrocarbon source rock for the Niger delta province (Evamy et al., 1978, Lambert-Aikhionbare & Ibe, 1984, Tuttle et al., 1999). The Akata shales are extensive across the whole region, whereas the turbidite sands are more localised as deep-water channel and lobe deposits.

These channel-lobe turbidites provide the principal deepwater reservoirs of Miocene age as well as the proposed Oligocene reservoir targets. Similar features are recognised through the Pliocene section as well as across the present day Niger Delta slope. Certainly, there is no evidence either from seismic interpretation or from borehole studies to suggest any significant change in sediment provenance or depositional processes between the Oligocene and Miocene systems. We are therefore confident in using what we know of the Miocene reservoirs as a template for understanding the Oligocene.

Tectonics and Structure

The end of Atlantic rifting in the Late Cretaceous gave way to gravity driven tectonism as the primary deformational process affecting delta development. Due to a rapidly prograding delta, low permeability, fine grained, pro-delta muds became over-pressured and formed mud diapirs as a response (Whiteman, 1982). Diapirism began in the Miocene and is still taking place today both at the delta front and extending further into the deep-water basin. The growth of the diapirs resulted in the development of growth faults, which offset the shallower parts of the section and flatten onto a decollement surface at the top of the hemipelagic muds. The overall structural trend is oriented in a northwest-southeast direction (Haack et al., 2000). Three structural provinces generally define the delta (Fig. 3): (a) an extensional province that extends from onshore to the outer shelf region, marked by large-scale listric growth faults; (b) a translational province across the upper and middle slope, dominated by mud diapirs and folds; and (c) a compressional province in the lower slope region, triggered by tectonic-scale downslope movement of sediment due to gravity gliding leading to toe thrust features and a marked fold and thrust belt (Bilotti & Shaw, 2005, Corredor et al., 2005, Deptuck et al., 2007).

METHODS

Petrography

Petrological analyses were conducted on 17 samples acquired from four wells in the study area. The cored samples were taken from the Miocene interval from Middle Miocene at a depth of approximately 2470m and lower Miocene at 3450m. Samples taken from depths shallower than 3000m were unconsolidated sands. The samples inspected were made into thin-sections and polished blocks as appropriate.
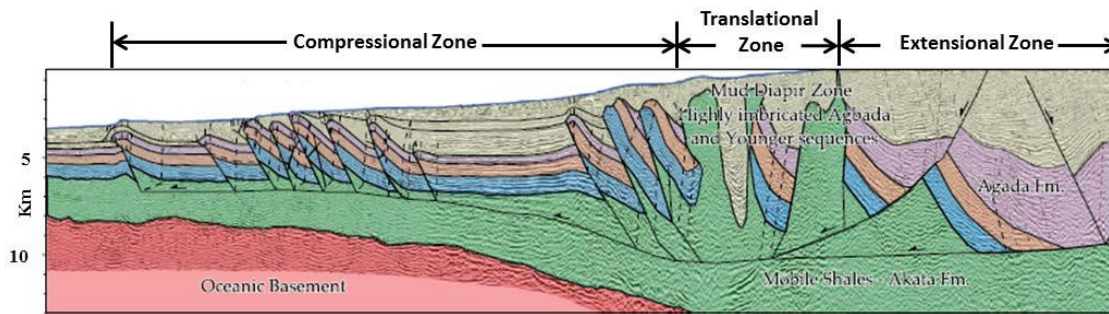
Fig. 3. Regional cross section showing the three structural provinces of the Niger Delta (modified from Corridor et al., 2005).

Techniques used included light optical microscopy and Scanning Electron Microscopy (SEM) using Back Scattered Electron imaging (BSE) and Cathodoluminescence (CL) analysis. Due to the poorly consolidated nature of most the samples (excluding the Lower Miocene samples), they were not suited for polished thin-sections; therefore thin-sections with cover slips were made. The samples were dried at 38°C and vacuum impregnated with epoxy resin to stabilise the samples. Ultraviolet glue was further applied to mount cover slips. For the purpose of SEM studies, samples were also made into polished blocks by drying at 38°C and placing in a 25/30mm diameter mould. The granular samples were filled with epoxy resin, mixed by stirring and placed under vacuum to remove air bubbles.

Optical microscopy was used for mineralogical identification and, where optical identification of quartz overgrowths was difficult, SEM was used. CL analyses were carried out on the SEM with a Centaurus CL detector. BSE and CL combined analysis was based on the method outlined by Evans et al (1994), which involves the analysis of pairs of BSE and CL images from polished block samples. A set of 13 samples were selected for this analysis. CL is particularly useful in distinguishing detrital quartz grains from syntaxial quartz overgrowths. SEM analysis was carried out over the Middle and Lower Miocene intervals to investigate the likely presence of microcrystalline quartz or chlorite rims, as they can impede the nucleation of quartz overgrowth if present (Bloch et al., 2002, Marchand et al., 2002, Taylor et al., 2010).

Petrophysical Analysis

Wireline log data from four wells within the study area were analysed to characterise the porosity and permeability of the reservoir zones penetrated. Of the four wells studied only one well penetrated the Oligocene interval. The density log was used to calculate porosity and these values were calibrated against core porosity where it was available. Permeability was estimated using the neural network technique, where sets of input logs (Gamma ray, sonic, density and neutron logs) were trained to recognise the core derived, stress corrected air permeability, acquired from routine core analysis (Sonde et al., 2011).

A multi-mineral model based on petrophysical elemental analysis (ELAN) of open-hole logs was used to compute the volume of mineralogical components within the intervals of interest. ELAN uses log curves and the response parameters of the tools to compute volumetric constituents of formation minerals and fluid. This method derives the relative quantities, or relative volumes, of the mineral components that would most probably produce the set of

measurements recorded by the logging instruments. The three-way relationship between tools (T), response parameters (R) and formation component volume (V) is shown in Figure 4.

Given the data represented by any two corners of the triangle (Fig. 4), the third can be determined. In this study, T and R are used to compute V. For quality control, forward modelling of R and V are used to reconstruct T – the input logs. The reconstructed logs are compared against the input data to determine the quality of the volume results. Four principal minerals (quartz, feldspar, zircon and kaolinite) were modelled in ELAN based on their abundances determined in the petrographic study.
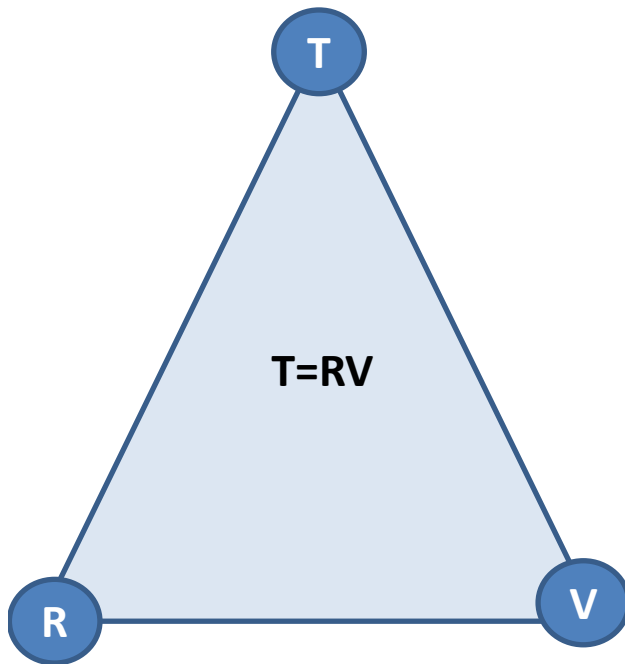

Fig. 4. Schematic illustration of ELAN. T represents the tool vector which in this case is the input log data (gamma ray, resistivity, neutron, density, and calculated porosity logs) and R is the response matrix which is a pre-defined value for the reading each tool would give for 100% of each formation component. R values were determined based on the known mineralogical responses to the physics of the different tools (Reeder et al., 2013) as defined using the Schlumberger Techlog software package. V is the volume vector which is the volume of each of the formation components.

Basin Modelling and Diagenetic Evolution

Since the early 1980's basin modelling has been used to study the burial and thermal evolution of a basin; particularly in relation to petroleum generation, expulsion, migration, accumulation and preservation (Welte & Yalcin, 1988, Wygrala, 1988, Talçin, 1991, Hermanrud, 1993, Underdown & Redfern, 2008). Basin modelling has also been used by some authors to study diagenetic evolution and to infer its impact on reservoir quality, particularly on porosity (Sombra & Chang, 1997, Walderhaug, 2000) by attaching a calculation of appropriate chemical reactions to the states generated by the basin model at different burial positions. Siever (1983) first associated chemical reaction calculations with fluid type and conditions, with stress and fluid pressure states and with temperature, permitting an estimate of the

transformation of organic matter to petroleum and also of quartz precipitation from a silica-rich fluid. Before the work of Siever (1983), the compaction models proposed by Athy (1930) were used to calculate porosity evolution using the degree of sediment compaction, but these relationships were not able to calculate the effect of porosity change due to cementation or dissolution. So starting with Siever (1983), models can relate calculated, or otherwise derived, basin history to temperature and to appropriate diagenetic reactions. However basin-modelling associated studies are certainly not the only method available to estimate paleo-thermal and paleo-chemical states. For example, paleo-temperatures have been regularly inferred from petrographic study of fluid inclusions, and particularly from chemical composition and isotopic signatures. Sombra and Chang (1987) follow this approach, using time-depth indices (TDI) to quantify the influence of burial history on the evolution of sandstone porosity.

Basin Modelling

The 2D basin model uses the transect shown in figure 3, oriented NE-SW and extending over 160Km across the extensional, translational and compressional parts of the Niger Delta basin (Bilotti and Shaw 2005, Corredor, Shaw et al. 2005, Deptuck, Sylvester et al. 2007; Figure 14). A total of seven chronostratigraphic horizons, the Seafloor, Lower Pliocene, Upper Miocene, Mid Miocene, Lower Miocene, Oligocene and Basement were digitized and used in this study. Each of the resulting defined units was assigned suitable lithologies. Where no well control was available, each lithology was initially assumed to be laterally continuous. Other basic requirements for modelling include boundary conditions, calibration data (corrected bottom hole temperature (BHT), vitrinite reflectance, pressure, porosity and present day hydrocarbon accumulations) and source rock properties, particularly the kinetic parameters that are responsible for the type and amount of generated petroleum. Interpreted faults on the 2D transect were also digitized, with priority given to the faults which are likely to have a significant impact on hydrocarbon migration. The fault selection method used adopted similar criteria to those chosen by Derks *et al.* (2012).

Quartz Cement Modelling

In this study the basin modelling tool used is PetroMod™ V.2013, which has an additional quartz cementation calculation module based on the Walderhaug quartz cementation model (Walderhaug, 2000). This module was well optimized with measured data (corrected bottom-hole temperature, vitrinite reflectance, pressure and porosity). Quartz cementation amount over the time-depth range represented in the basin model was then calculated. However, Walderhaug (2000) expressed the effect of cementation as a function of change in quartz surface area whereas PetroMod™ models cementation as a function of porosity loss rate. Equation 1 shows the relationship expressed by the Walderhaug quartz cementation model

$$A = (1 - C) 6 f V \phi / D \phi_0 \qquad\qquad (1)$$

where A is change in quartz surface area, C is the fraction of quartz grain surface coated by clay or other substances, f is the volume fraction of quartz clasts, V is the sample volume and D is the average quartz grain diameter. PetroMod™ uses the cementation equation shown in equation (2). Both cementation modelling algorithms vary with assigned detrital mineralogy, quartz grain size, quartz grain coating abundance, temperature and quartz surface area. The porosity loss rate due to quartz cementation that has been adopted in PetroMod™ is therefore expressed as:

$$\frac{\delta \phi cc}{\delta t} = \frac{m}{\rho} \frac{(1-C)6f}{D} \frac{\phi}{\phi_o} A e^{-Eo/RT}$$

(2)

where C is the quartz grain coating factor, f is the quartz grain volume fraction, D is the average quartz grain diameter, A and E_o are respectively the frequency factor and activation energy of quartz precipitation. M represents the mole-mass and ρ the density of quartz (Walderhaug 1994).

The average grainsize and quartz grain volume fraction used in the quartz cementation calculations were based on the results of the petrological study. A dominant grain size range of 125 - 500μm is seen in the Miocene. No core has yet been taken from the Oligocene interval. So, in the absence of any grainsize measurements, it was assumed that the Oligocene reservoirs in the study area, which are below 3800m, would have a similar grain size as the Lower Miocene reservoir at 3450m, the deepest cored section available to this study.

The PetroMod™ calculation assumes that quartz is sourced by stylolitisation. In addition, it is also assumed that the precipitation phase of the overall quartz dissolution, transportation and precipitation process is the slowest and hence the rate-controlling step in the entire process (Walderhaug, 2000).

By Implementing the Walderhaug quartz cementation model as part of the simulation, the percentage pore space occluded by cement was estimated. The results show that cement volume tends to increase both with depth and landward and up-dip along the regional transect (Fig.15) as water column thickness decreases and mean overburden increases. Little or no cement is predicted above 3000m but cementation starts to develop from about 3450m depth within the Lower Miocene reservoirs with less than 5% of the pore space now containing quartz cement. The cement volume increases steadily with depth into the potential Oligocene reservoirs with values of close to 14% of pre-cementation pore space. The minor quartz cement observed from the petrographic study for the Lower Miocene reservoir and the absence of quartz in Mid-Miocene agrees with this modelled result. The modelled result is also displayed as a 1D extraction at the well location from the 2D model with cement volume plotted against depth (Fig.16).

RESULTS

Miocene Sediments

The Miocene reservoirs in the study area are typically composed of loosely consolidated sands that are moderately sorted and display a dominant grain size of medium to fine, although coarser grain sizes also exist. The sands have been classed as quartz arenites (McBride, 1963) as they are largely composed of quartz with less than 15% feldspar and minor lithic component (< 2%). The excellent quality of the reservoir sands is largely attributed to the unconsolidated nature of the sands with little or no cementation present.

A total of 15.1m of cores was studied; 12m across the Mid-Miocene and 3.1m across the Lower Miocene sequence. The Mid-Miocene reservoir facies comprise massive, unconsolidated sands that are typical of the Bouma Ta facies, with minor normal grading seen in the sands. High density turbidity current flow is the most likely depositional mechanism. Two

facies have been noted in the Lower Miocene; (1) light grey, very fine consolidated massive sands that are moderately to well sorted, representing deposition by high density turbidity currents, and (2) interlaminated very fine sands and silts characterised by millimetre-scale parallel and convolute lamination. Some dark laminations are also noted and are most likely mud or organic material. These facies most likely represent dilute turbidity current deposition. Fig. 5 is a schematic diagram of the sedimentological log of the core section studied, with representative core photographs of facies where samples for petrographic analysis were taken.
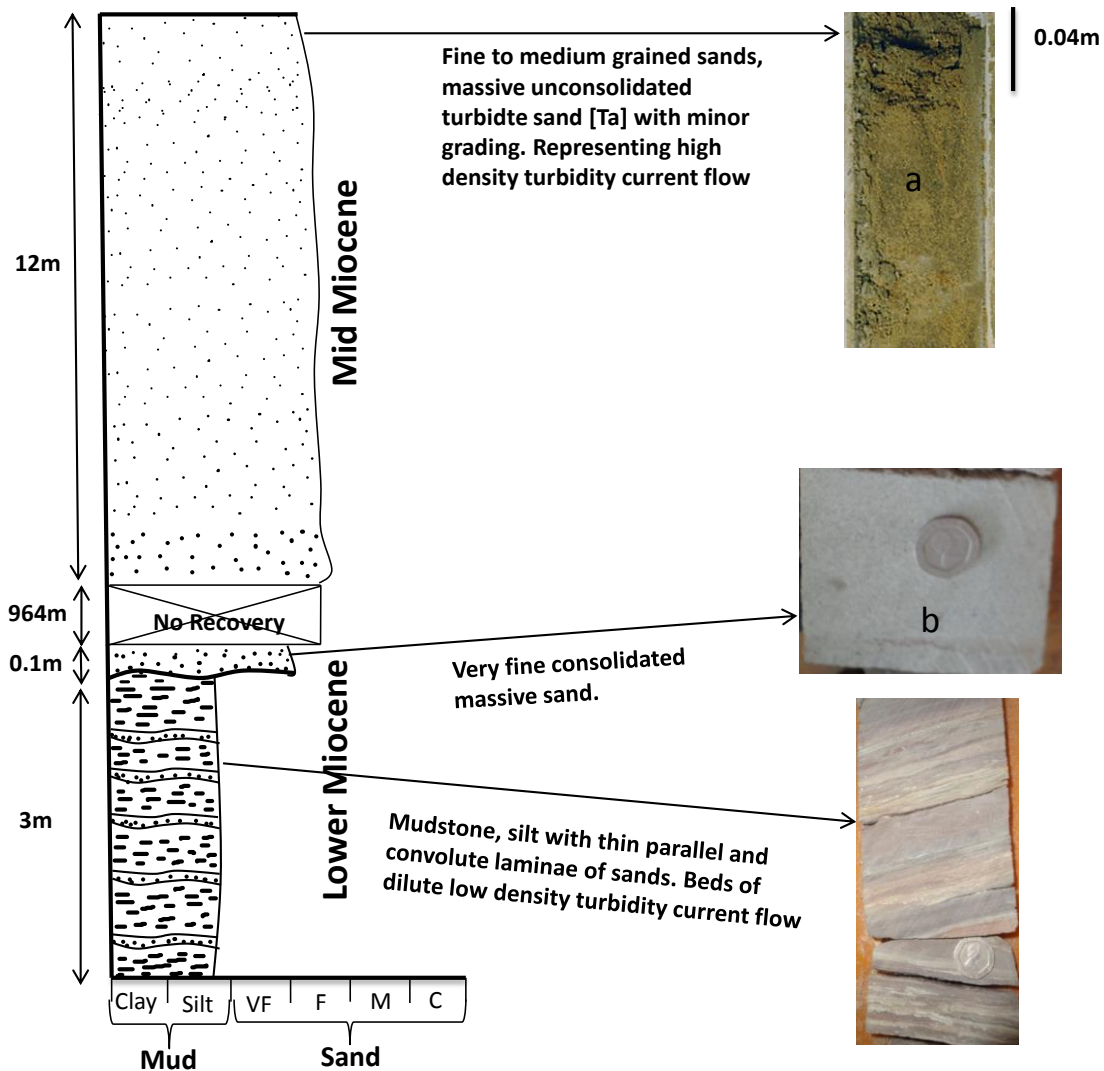
Fig. 5. Sedimentological log of core from well A1 across the Mid Miocene and Lower Miocene sections. Core photos represent typical examples of the lithologies described; petrographic samples were taken from 'a' and 'b'.

Petrological Analysis

Detrital Mineralogy

The Miocene samples from the three wells examined by optical microscopy are composed dominantly of quartz, comprising up to 85% monocrystalline grains, with minor polycrystalline quartz, 10% feldspar and 0-5% lithic fragments of possible igneous and metamorphic origin

(Fig. 6). Muscovite and heavy minerals (probably zircon) occur in trace amounts. Heavy minerals are easily recognisable using the SEM micrographs as highly luminescent grains, as depicted in Figs. 7A-D. Grain size ranges between fine and medium sand (125 - 500 microns), with sorting from poor to well-sorted and grain roundness from subangular to angular.
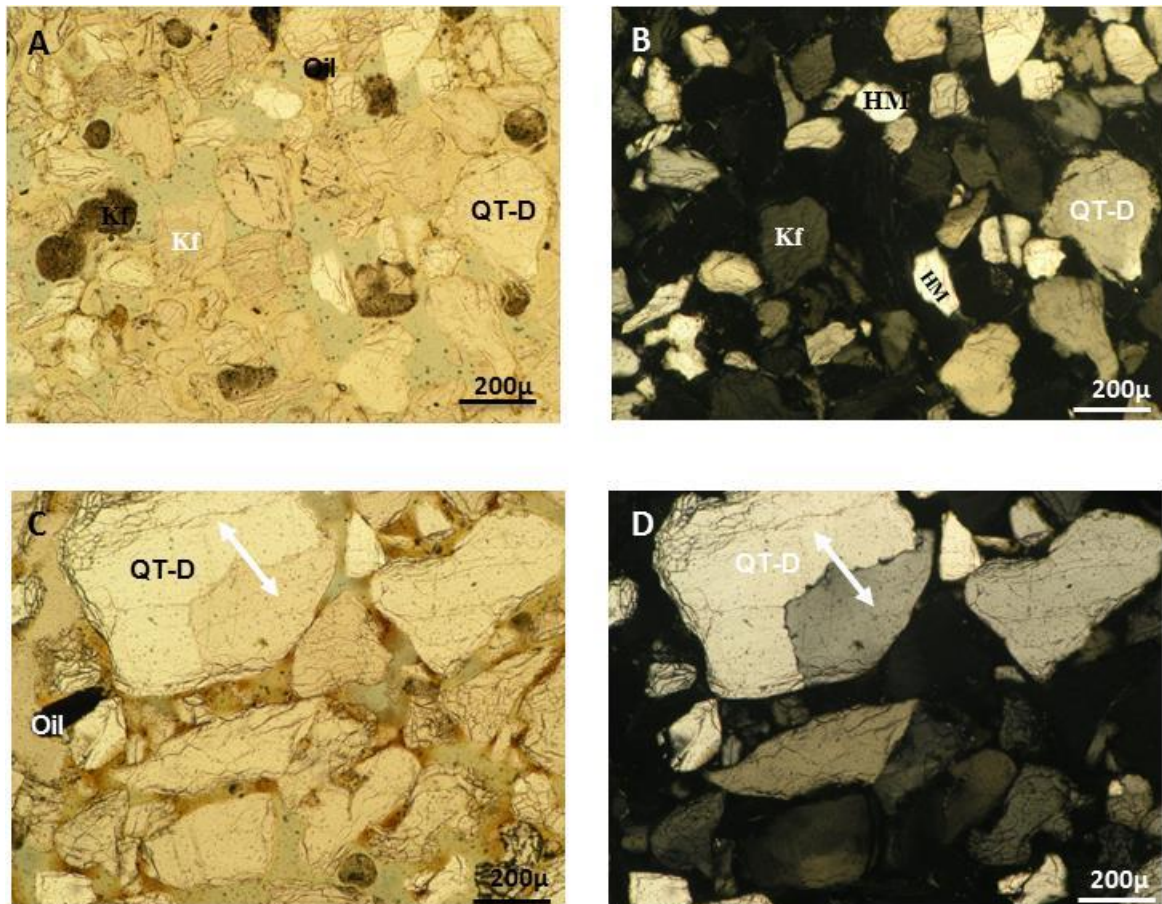

Fig. 6. Photomicrographs in both plane polarised light and cross polars of Mid-Miocene (A, B) and Lower Miocene reservoirs (C, D), (detrital quartz (QT-D), K-feldspar (Kf), polycrystalline (arrows)).

Diagenetic Mineralogy
Quartz Cement: Quartz cements are rarely observed in thin-sections in the Mid-Miocene samples located at depths of less than 3000m. However, thin-sections of samples retrieved from the Lower Miocene reservoirs at 3450m, do show some quartz overgrowths. In some cases, they occur as euhedral overgrowths protruding into primary pores. The overgrowths range in size from individual small euhedral crystal growths of 3-20μm to grain-rimming cements of less than 30μm thick. Overgrowths are not widespread but are locally developed around quartz grains. CL and BSE analyses allowed distinction between authigenic and detrital quartz. Authigenic quartz rims are typically less luminescent than their detrital host (Fig.7D). SEM images reveal quartz overgrowths with well-defined crystal faces over the surface of the detrital host (Fig.7E). BSE analyses of the same sample showed no distinction as both detrital and authigenic quartz display the same false colour grey (Fig. 7C).
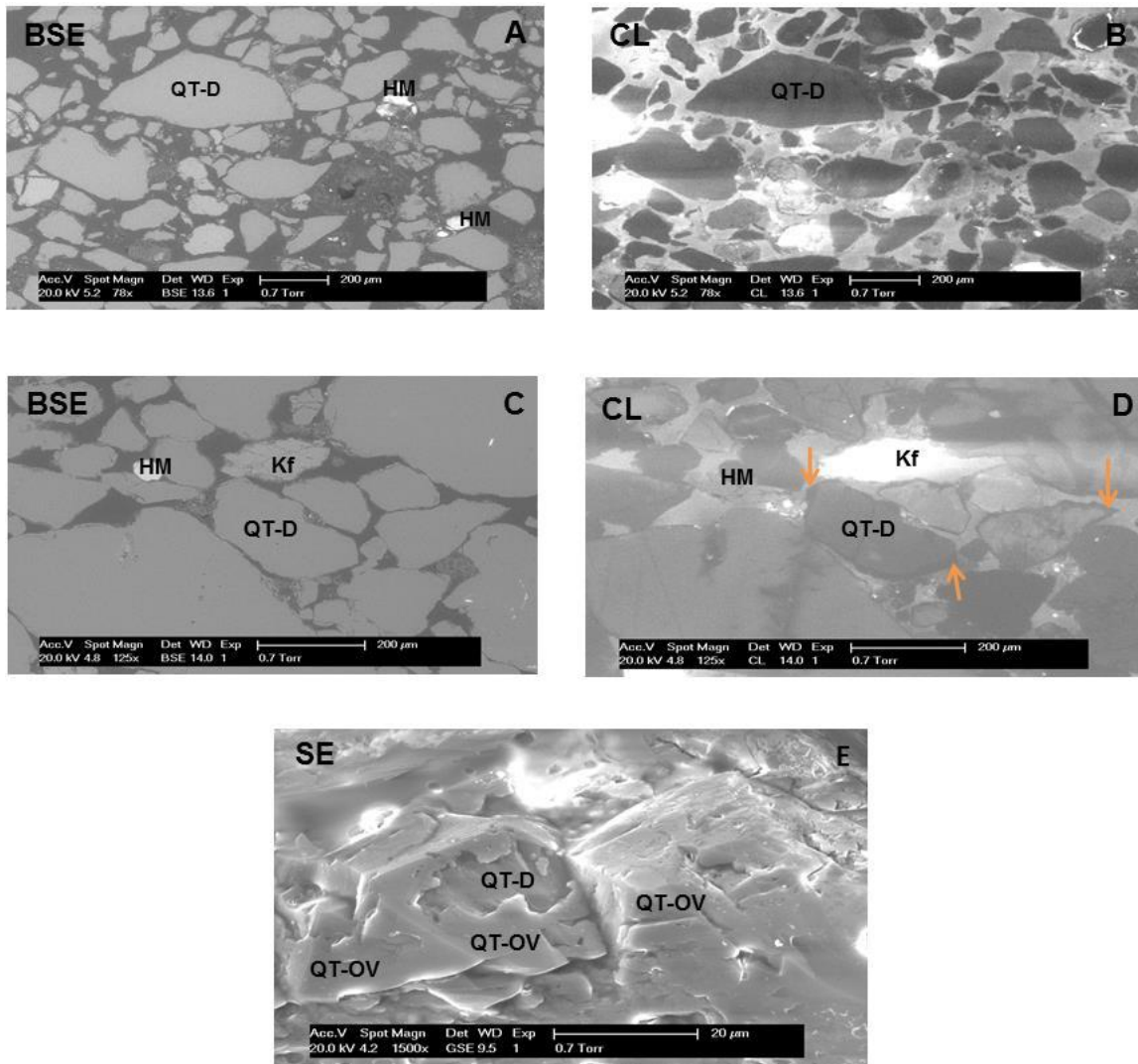
Fig. 7. Upper Miocene polished block samples with no quartz cement seen from both BSE and CL plates (A and B), while overgrowths (indicated by amber arrow) are present in the Lower Miocene samples (C, D and E), (detrital quartz (QT-D), quartz overgrowth (QT-OV), K-feldspar (Kf), heavy mineral (HM)).

Grain Coating: The SEM analysis of the samples does not reveal the presence of any grain coating minerals of early origin. The upper Miocene samples are seen, however, to be coated with thick 'dead'/bituminous oil (Fig. 8). The presence of this oil is indicative of biodegradation due to exposure of the Mid-Miocene reservoir to temperatures of less than 60° C (Peters et al., 1996).

Clays: SEM examination revealed the presence of kaolinite-type clay in both the Upper Miocene and the Lower Miocene successions. These clays occur as stacked pseudo-hexagonal crystals of euhedral booklets (Fig. 9A and B). In the Lower Miocene succession, kaolinite is observed choking primary intergranular porosity, suggesting that the kaolinite clay developed before the main phase of mechanical compaction (Gier et al., 2008 Fig. 9C).
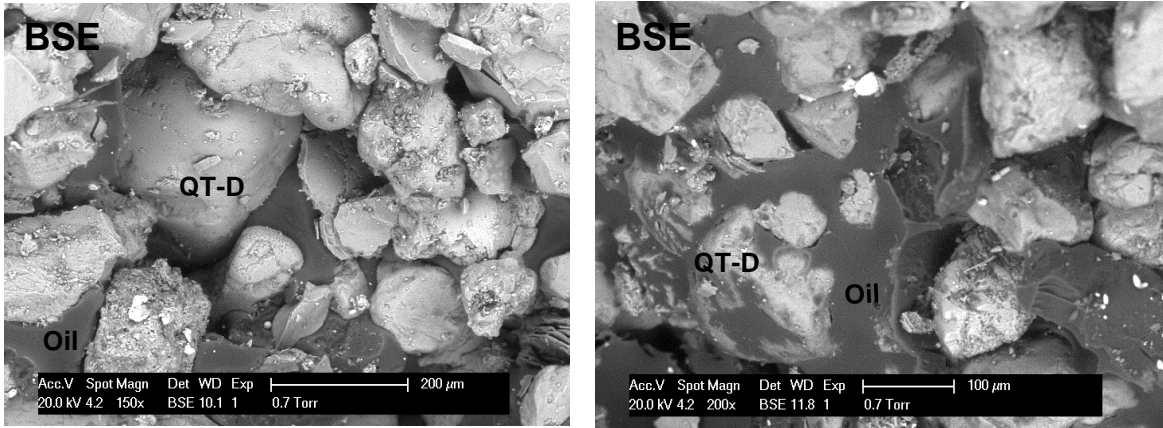
Fig. 8. BSE image of Upper Miocene samples showing quartz grains surrounded by oil.
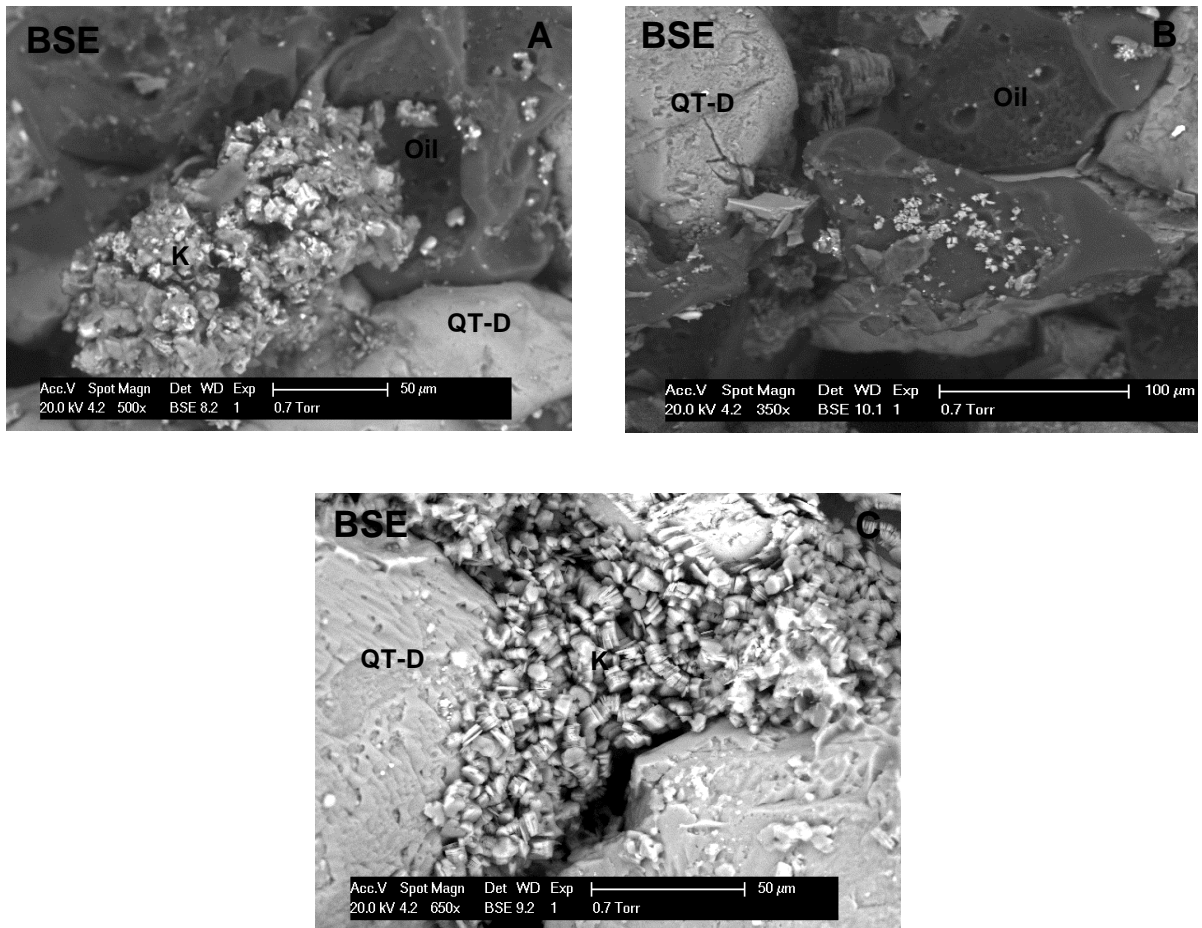

Fig. 9. BSE images of Upper Miocene and Lower Miocene Sandstones. A and B images show authigenic kaolinite surrounded by oil, (C shows pore filling kaolinite crystals: (detrital quartz (QT-D), quartz overgrowth (QT-OV), oil, kaolinite (K)).

Petrophysics

The calculated porosity from wireline log analysis (for example in Fig. 10) decreases with depth as seen from the porosity depth plot of 4 wells in the study (Fig. 11). The Figure also reveals that only the estimated porosities from Well A1 (represented by a triangle), which is
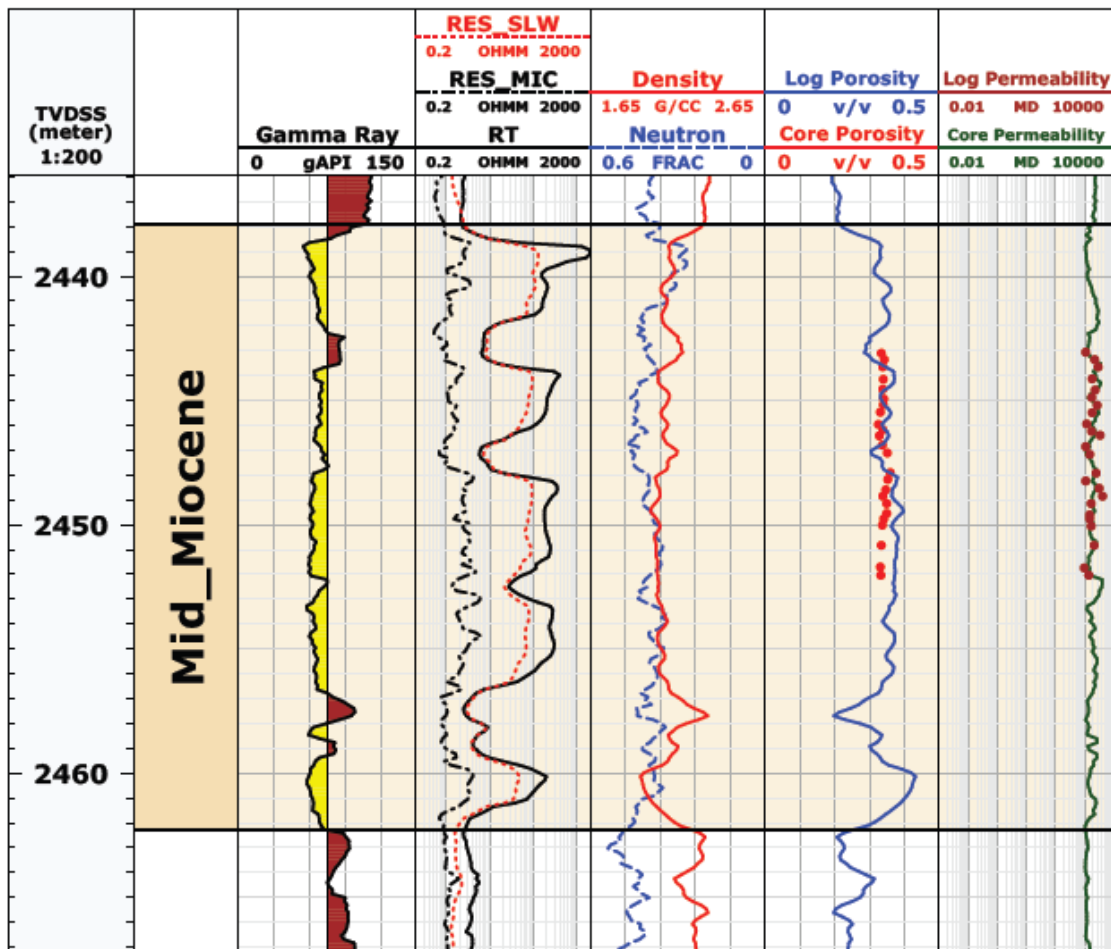

Fig. 10. Petrophysical data log showing modelled porosity calibrated to core porosity (track 6) and modelled permeability calibrated against core permeability (Track 7).

the only well that encountered the Oligocene reservoirs have average porosity values of 20 % .The porosity for the Miocene, generally ranges from 21- 37% across all the wells, (see Fig. 11).

The results of the multi-mineral analysis are displayed in Fig. 12. Tracks three to seven of Fig. 12A show the input logs while the last track shows the multi-mineral model derived from the open-hole logs. The modelled quartz volume is seen to increase with depth as observed from the cross plot of quartz volume as a fraction of the total reservoir component (mineral, fluid and rock) plotted against depth (Fig. 12B) with two trend lines seen. However, it is not possible to verify the proportions of detrital and authigenic quartz from the multi-mineral model. The first trend line 'a' indicates a steady increase with depth in quartz volume of close to 60% volume fraction from the Upper Miocene to the Middle Miocene reservoirs. An offset is seen in the second trend 'b' representing quartz volume for Lower Miocene down to the Oligocene with an estimated quartz volume of close to 80% in the Oligocene reservoir intervals.
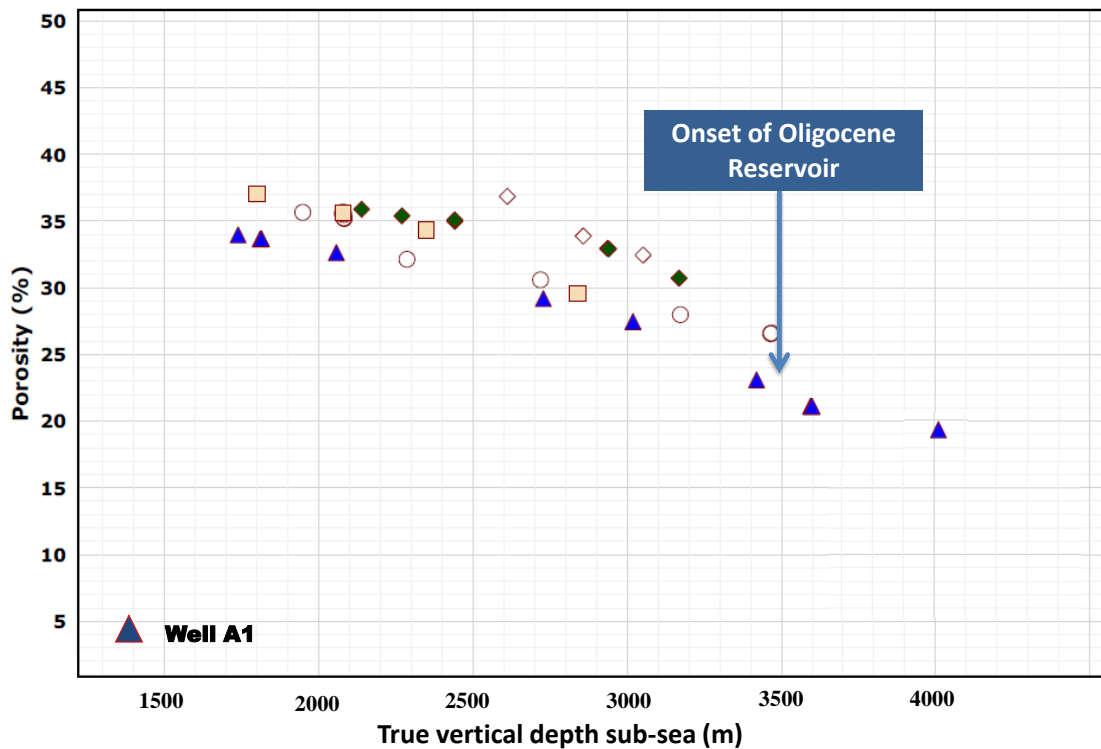
Fig. 11. Porosity-depth trend showing a reduction in porosity for several stacked reservoirs plotted against depth for 4 wells. Well A1, the deepest well, highlighted in blue triangles with Oligocene porosity starting at 3500m.

Basin Modelling

### *Temperature and Pressure History*

The thermal history calculated by the 2D basin model shows that the Mid-Miocene and younger reservoirs in the study area have never been exposed to temperatures above 60° C (Fig. 13a), which is below the 70-135° C initiation of effective quartz precipitation temperature range (Walderhaug, 1994, Bjørkum et al., 1998). On the other hand both the Lower Miocene and the Oligocene intervals are calculated to have reached temperatures above 70° C. The Oligocene has been exposed to temperatures above 70° C from the Early Miocene (19Ma) to the present (reaching 90° C in the Mid-Miocene and 120° C by the Pleistocene, Fig. 13A). In contrast the Lower Miocene reservoirs encountered temperatures at and above 70° C from the Early Pliocene, reaching about 80° C at the present day, which can explain the very minor quartz overgrowths observed in samples of this age. It is well established that overpressured reservoirs retain porosity because mechanical compaction is inhibited (Taylor et al., 2010).

The simulated pressure history of the reservoirs indicates that the Miocene reservoirs have not developed overpressure, but that the Oligocene rocks did encounter overpressure from the Mid-Miocene, the overpressure value having continued to increase to the present day having a value of about 12MPa, as seen from the separation of the modelled pore pressure (PP) and hydrostatic pressure (H) lines (Fig.13B). Notwithstanding, the over-pressured Oligocene sandstones are not likely to have avoided all quartz cementation because they were exposed to temperatures high enough for cementation from the Early Miocene (19Ma), which

is prior to the significant Late Miocene (10Ma): the temperature for quartz cementation was reached 9 Ma before overpressure developed.

Quartz Cement Modelling

By Implementing the Walderhaug quartz cementation model as part of the simulation, the percentage pore space occluded by cement was estimated. The results show that cement volume tends to increase both with depth and up-dip (Fig.15) as water column thickness decreases up-dip and mean overburden increases. Little or no cement is predicted above 3000m in the area of Well 1A but cementation starts to develop from about 3450m depth within the Lower Miocene reservoirs. In sandstones at this depth, less than 5% of the pore space has been occluded by quartz cement. The cement volume increases steadily with depth into the potential Oligocene reservoirs where values of close to 14% occlusion of pore space are reached. The minor quartz cement observed from the petrological study for the Lower Miocene
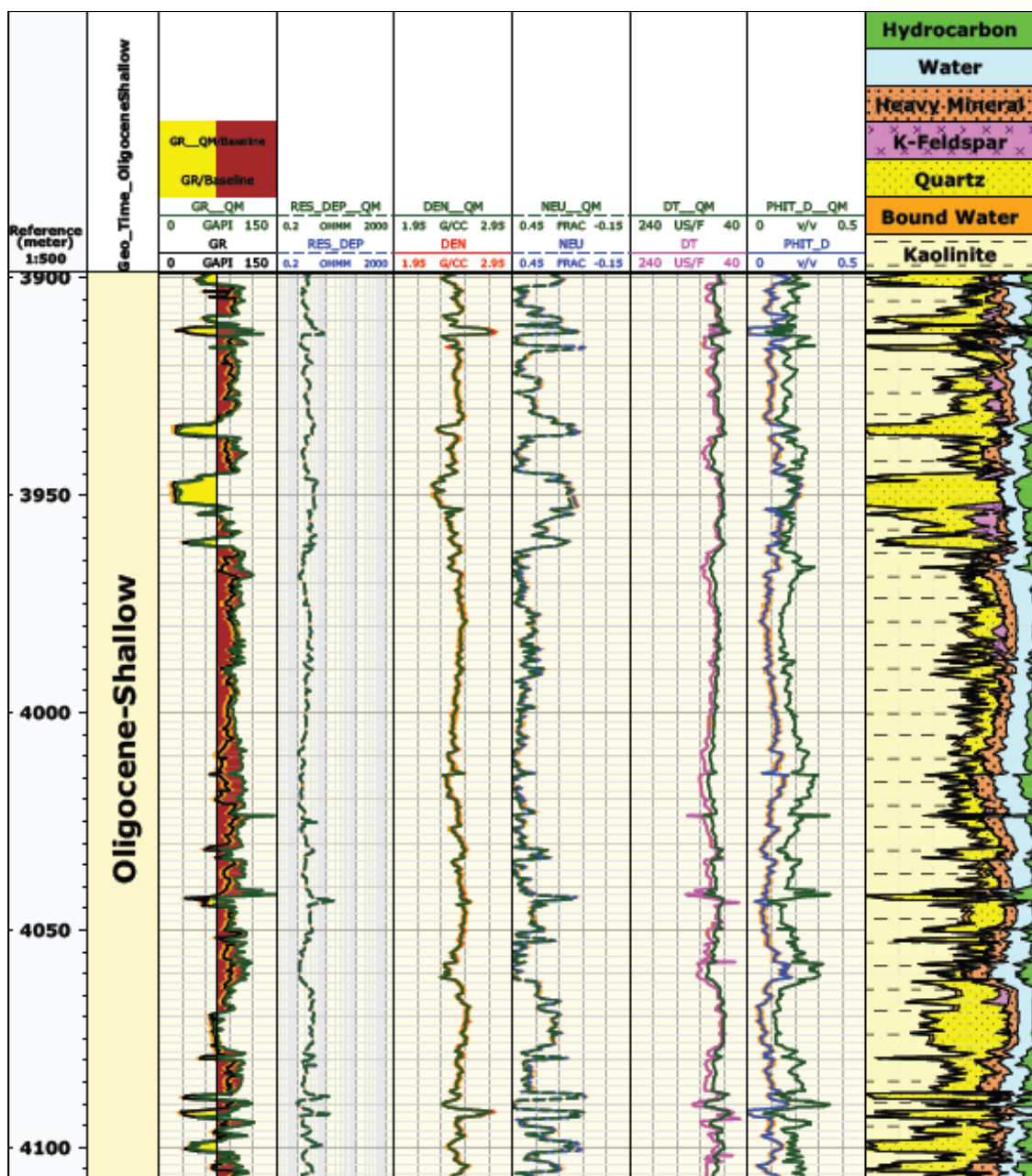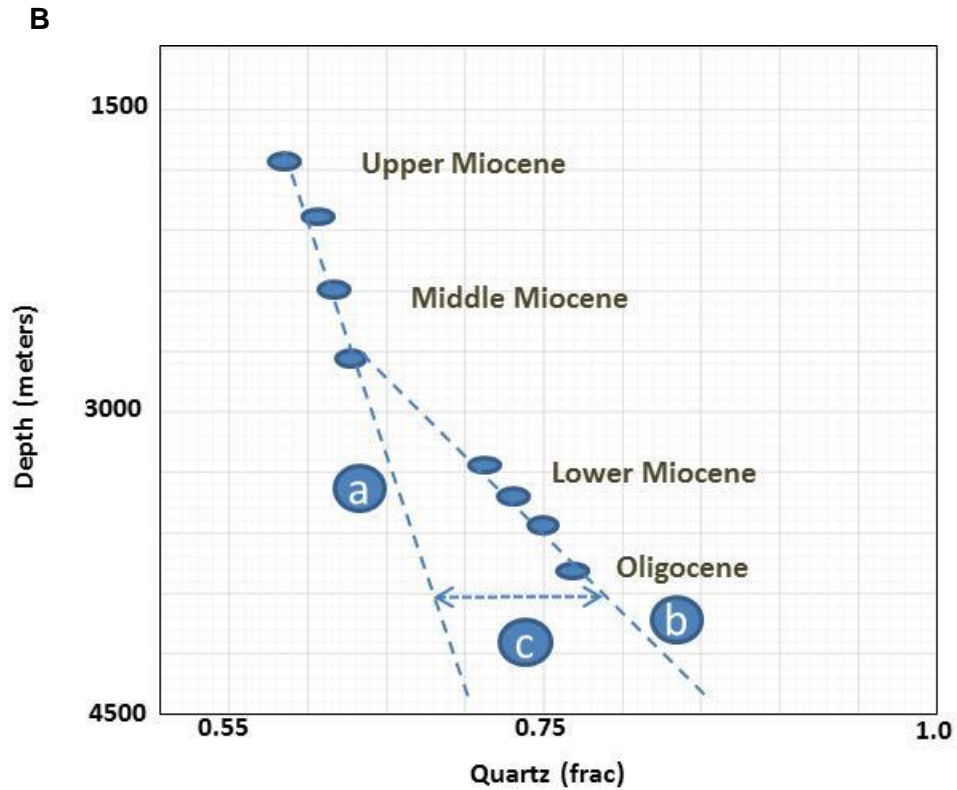
B

Fig. 12. (A) Modelled mineral volumes in Track 8 (quartz=yellow, feldspar=pink, mica=black, kaolinite= cream with dash).Track 3; Gamma ray, Track 4;resistivity;Track 5; density, Track 6; neutron and Track 7; porosity. Logs with the suffix ELAN represent back calculated logs: B) Cross plot of modelled quartz volume against depth.

reservoir and the absence of quartz in the Mid-Miocene reservoir agrees with this simulated result. The simulated result is also displayed as a 1D extraction at the well location from the 2D model with cement volume plotted against depth (Fig.16).

The trend observed in the quartz model also closely resembles the trend from the multi-mineral analysis of Fig.12B. A corresponding decrease in modelled porosity from Miocene to Oligocene reservoirs is seen when the modelled porosity is plotted against depth. A good match is seen between the modelled porosity and the average calculated porosity from the well log (Fig.17).

A 1D (column) that was extracted from a 2D basin model near the deepest well, shows the volume fraction of pore space filled with quartz cement plotted against depth (see Fig.16). The figure shows an increase in cement with depth as is expected; a similar trend is predicted from multi-mineral petrophysical evaluation, where major rock mineral volumes have been estimated from well log responses. A good match is seen between the original input log and the reverse calculated versions of the logs with a suffix of ELAN attached to the name of the curve (Fig.12A). This is a good quality control for the estimated volumes of quartz, feldspar, zircon and kaolinite.
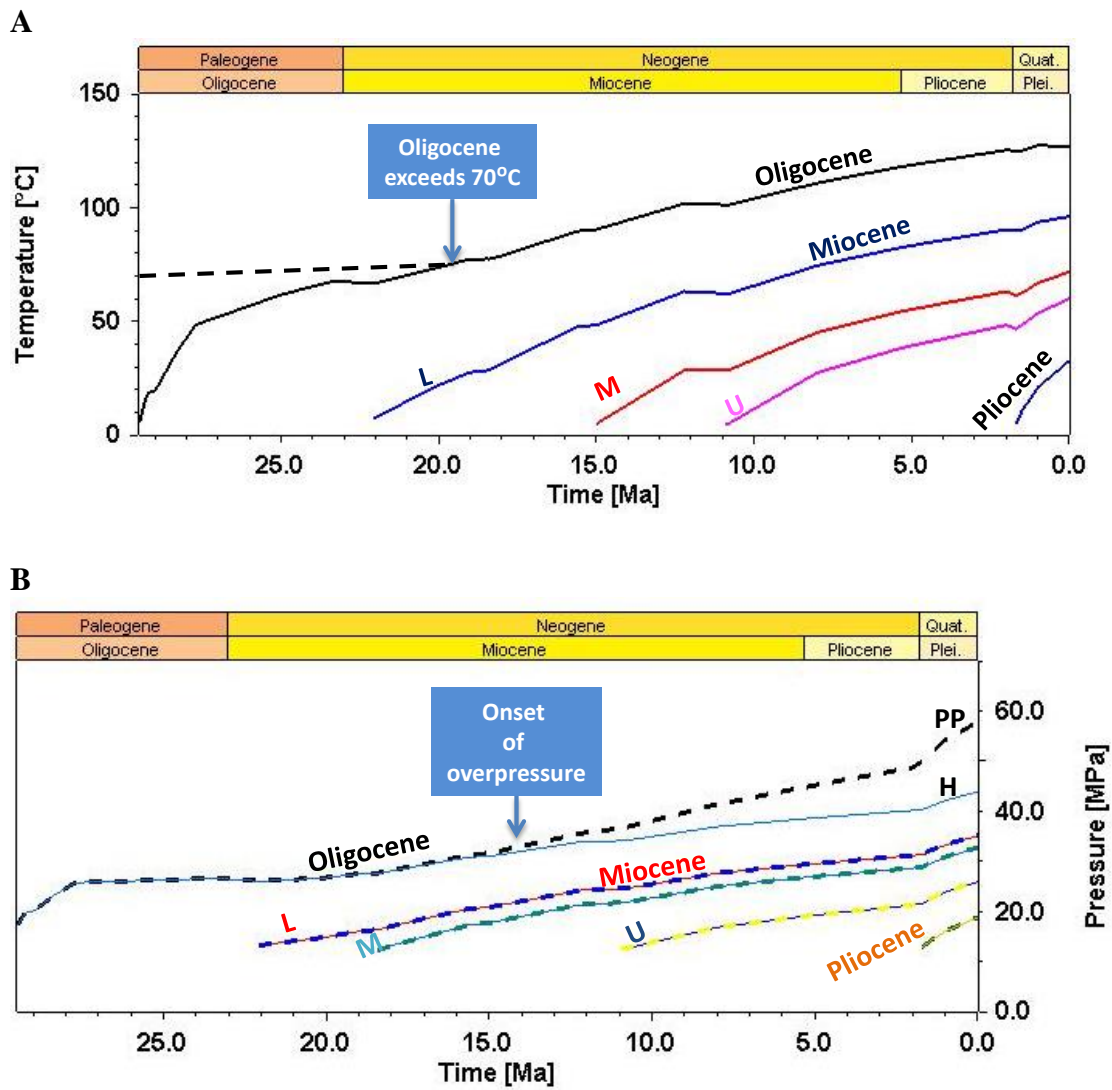
Fig. 13. Modelled thermal (A) and pressure (B) history. The pressure histories (B) are plots for both hydrostatic (line) and pore pressure (dash): (L=Lower Miocene, M= Middle Miocene and U= Upper Miocene).

A cross plot of the fraction of quartz volume against depth shows an increase in quartz with depth. There is a clear demarcation of two trends, a higher gradient down to the Mid-Miocene (trend 'a') and a gentler gradient from Lower Miocene down to the Oligocene (trend 'b'). It is not possible to differentiate between detrital and authigenic quartz as contributors to the total quartz as indicated on this plot. However, if we assume a stable sediment supply yielding a constant quartz volume input, then trend 'a' can be interpreted as a function of physical compaction due to the weight of the overburden, such that the quartz volume increases slowly and steadily as a percentage of the total rock volume. Whereas the second trend 'b' shows a more rapid increase of quartz volume with depth, which can be interpreted as a function of both compaction and quartz volume increase due to cementation. The separation of trend 'a'
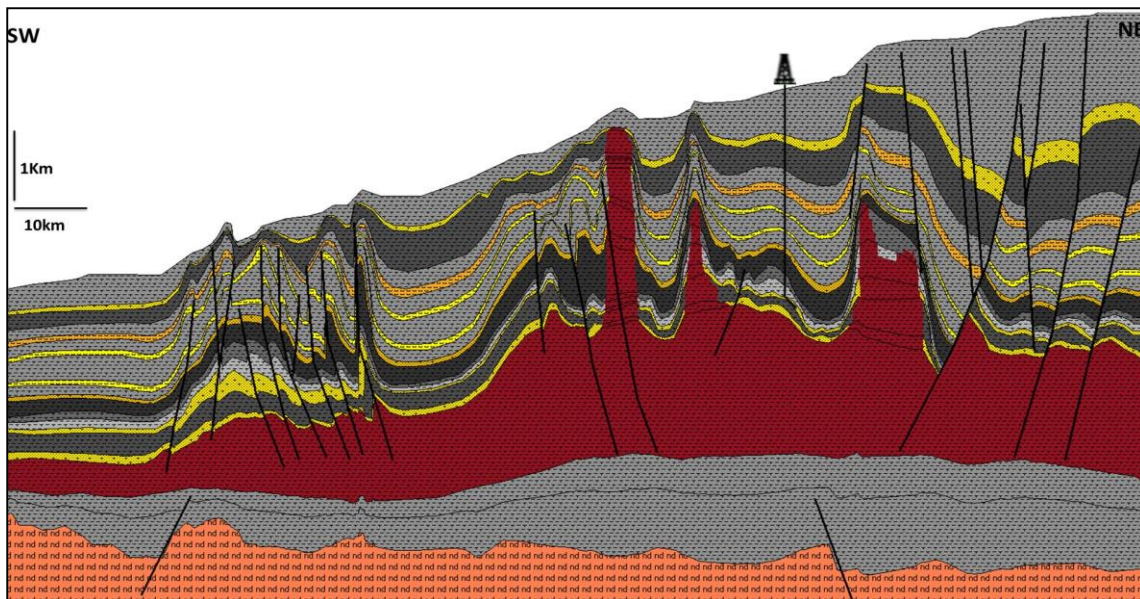
A
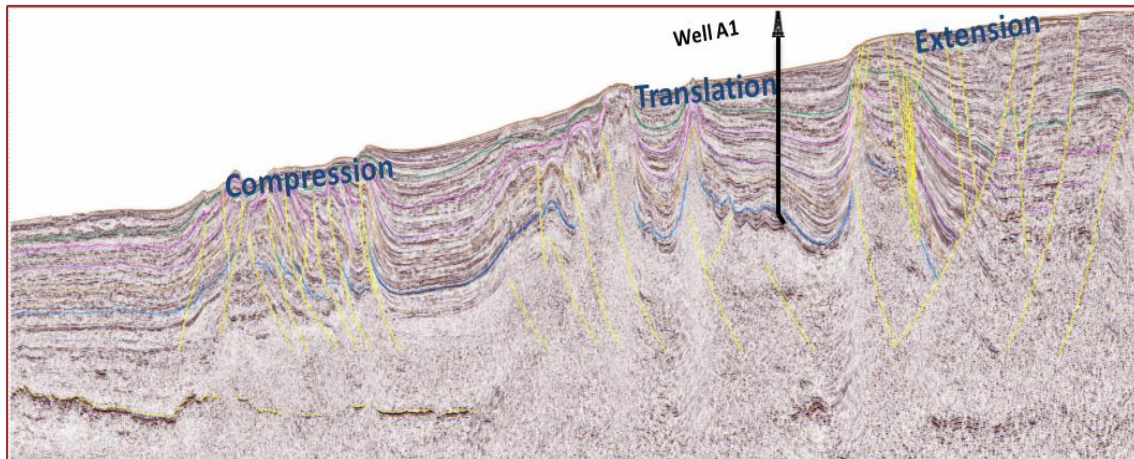
B

Fig.14. A = interpreted regional 2D transect across the 3 structural provinces; B) Digitized 2D transect.

and 'b', designated as line 'c', can be assumed to be additional quartz volume of about 10% due to quartz cement. This assumption is supported by: (1) the modelled quartz cement that is based on the Walderhaug algorithm which shows an onset of quartz cementation from the Lower Miocene, increasing volumetrically in the Oligocene to a quartz cement volume of less than 14% (Fig.16); and (2), the presence of quartz overgrowths noted from the petrographic inspection of the Lower Miocene samples (Fig.7D and E). No quartz cement was seen in samples from shallower or younger reservoirs.
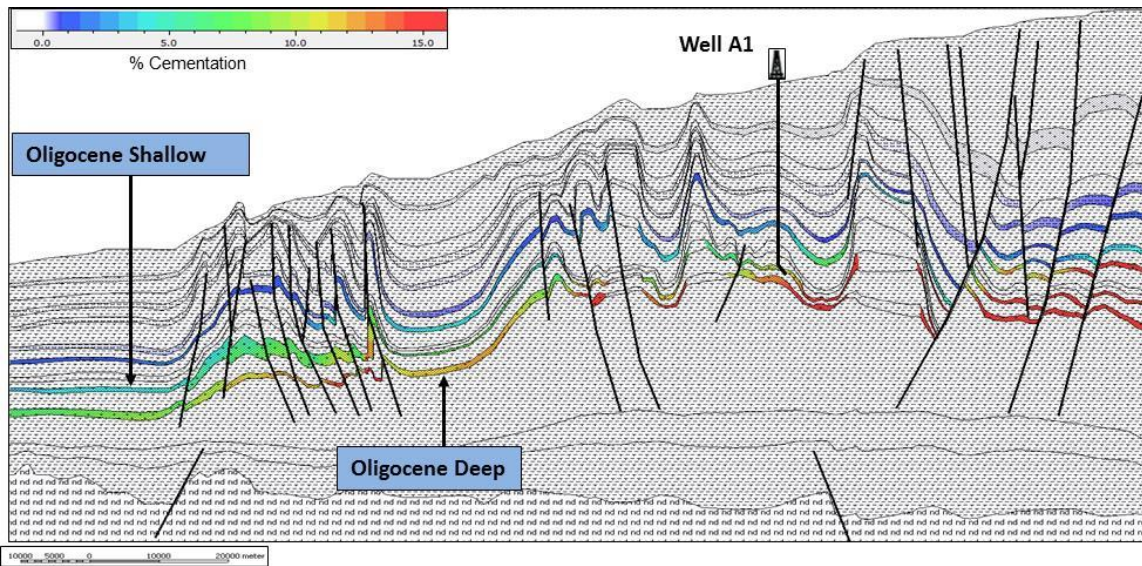
Fig. 15. Overlay of predicted quartz cement on 2D transect. Colour spectrum show increase in cement volume from blue to red. In the vicinity of well A1 cement volume increase with depth from Miocene to Oligocene.
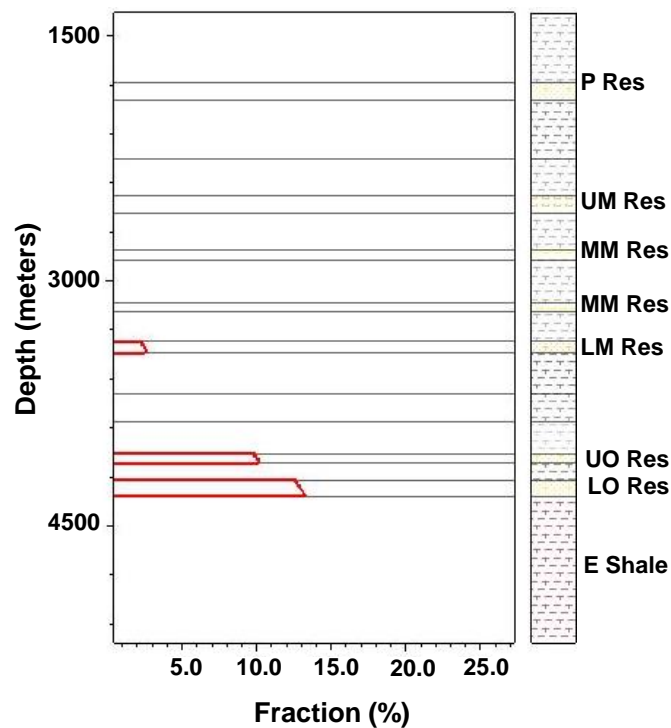
Fig. 16. Fraction of pore space occluded by quartz cement plotted against depth: a 1D extract from the 2D model in Fig. 11. (Res =reservoir, P =Pliocene, UM = Upper Miocene, MM = Mid-Miocene, LM = Lower Miocene, UO = Upper Oligocene, LO = Lower Oligocene, E = Eocene).

DISCUSSION

The focus of this work is to better understand the reservoir potential of the Oligocene interval buried below 3800m, most importantly how, and to what extent, quartz cementation has reduced porosity below that attributable to the depositional character and mechanical

compaction with burial. The burial-related mechanical compaction, temperature and pressure histories have been calculated by basin modelling and have then been used to calculate probable amounts of quartz cementation throughout the burial history, given the sediment properties such as quartz content and grainsize that are known to control cementation rate.

There is direct evidence of some quartz cementation at the lower Miocene. CL images of samples from the deepest cored Lower Miocene interval at 3450m reveal the presence of syntaxial quartz overgrowths (Fig.7D and E). However the overgrowth is less than 30μm thick, suggesting that the effect on porosity here is likely to be minimal. This expectation is supported by the porosity calculated from density logs for this interval, which shows an average value of about 25% (Fig.11). This value is consistent with only mechanical compaction. The presence of quartz overgrowths in the Lower Miocene is taken as indicative of an increase in cementation with depth and consequently the potential for a significant degree of quartz cementation within the Oligocene reservoir. There is, however, no direct evidence from the Oligocene, so quartz cementation calculations require a critical assessment of the assumed parameters.
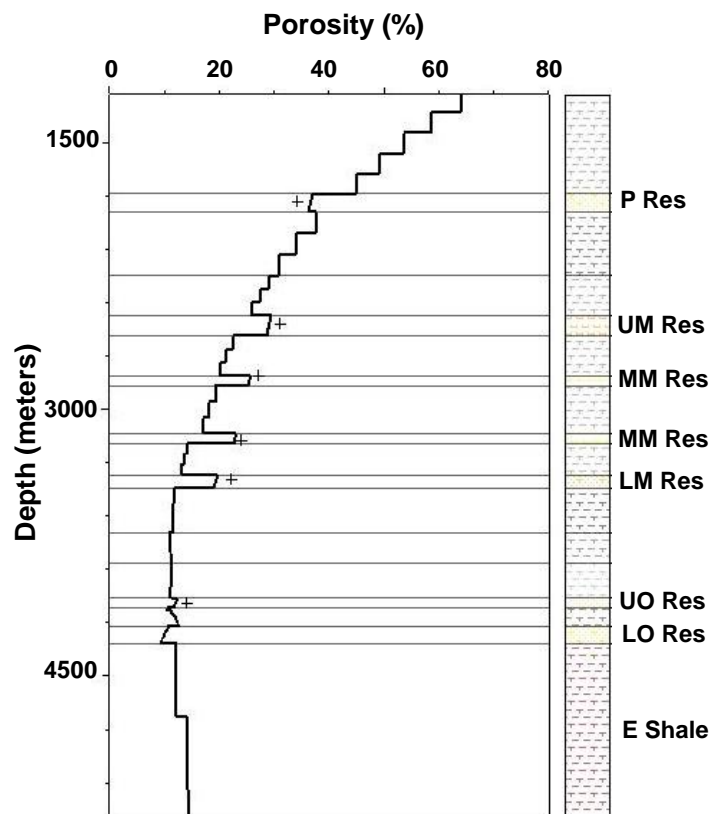
Fig. 17. Modelled porosity (black line) versus depth calibrated against calculated porosity from well log (black cross). (Res = reservoir, P =Pliocene, UM = Upper Miocene, MM = Mid-Miocene, LM = Lower Miocene, UO = Upper Oligocene, LO = Lower Oligocene, E= Eocene).

The main parameters that control quartz cementation rate as calculated here are mineralogy, grainsize and degree of grain coating, together with temperature, pore fluid pressure and

particularly its deviation from the hydrostatic, and potentially the presence of petroleum. These are discussed below for the Oligocene, recognising the degree to which the values are known.

Mineralogy: The Oligocene has not been sampled directly so we must make an estimate of the likely mineralogy based on an assessment of the overlying Miocene succession. There is no reason to assume that sediment supply to the deepwater varied significantly during this time interval, as the provenance and supply routes have not changed, so we can use values taken from the Miocene. This is true throughout the Miocene section, as well as into the Pliocene. The sandstone turbidite reservoirs of Miocene age are all quartzarenites (i.e. > 90% quartz by weight). Assuming a depositional porosity of 40% by volume, we have calculated an initial volume percent of 54% quartz, which we have used in the quartz cementation calculations. There is a general absence of calcite and relatively low percentages of clay minerals, so that we would not expect marked cementation or pore-clogging by other authigenic minerals.

Grain size: Following a similar reasoning and based on an average of the range of mean grain-size values found in Miocene reservoirs, we have assumed a value for the Oligocene sands of 0.12mm, i.e. fine-grained sandstone. It is interesting to compare with other turbidite reservoirs of similar age. In the Lower Congo Basin, for example, field data indicate that the petroleum bearing Oligocene reservoirs have grain sizes that vary from very fine to very coarse grained (0.125mm-2mm) (Dessus and Abreu 2002, Pelleau, Serceau et al., 2002, Delattre, Authier et al., 2004). The Oligocene reservoirs of the Campos Basin are mostly medium to coarse grained (0.25mm -1mm) (Souza, Scarton et al., 1989, Pinto, Antonio et al., 2001, Bruhn, Gomes et al., 2003). In our model calculations, different input grain sizes have a significant effect on calculated quartz cementation amount. A grain size of 0.05mm (coarser silt) produced 19% of the pore volume filled with cement whereas a grain size of 2mm (very coarse sand) produced a cement volume of 1.8%. It is possible that the Oligocene sands may have been deposited in a marginally more distal slope setting. Indeed, there is evidence from our interpretation of depositional environments that the Oligocene reservoirs represent deposition in ponded mid-slope lobes whereas the Miocene reservoirs are inferred slope channel deposits (Chudi, 2015; Chudi et al, in press). However, it is unlikely that the very slightly finer grain size for the Oligocene sandstones would make more than 1-2% difference in occlusion of porosity by quartz cementation.

Grain coating: In this study, the Miocene samples observed in SEM and under the optical microscope did not show any evidence of grain coating; this was true for all samples studied including those from the earliest Miocene. However, in order to assess sensitivity to coating, we systematically increased the grain coating value in our model from 0 to 100% and as coating percentage increased the calculated volume of quartz cement decreased steadily. Full (100%) grain coating (perhaps unsurprisingly) completely inhibits cementation, yielding no cement, whereas a complete absence of grain coating favours cementation, and yielded up to 14% of pore space occluded by cement. The evidence we have favours the latter figure as more likely to be representative of the Oligocene section.

Temperature: Temperature is calculated directly in the basin model as is pore pressure, together with its deviation from the hydrostatic pressure gradient. These values have been used to calculate the degree of quartz cementation. Sensitivity studies have also been

performed around these values to accommodate reasonable variations either side of the basin simulation results. The heat flux history within this passive margin was modelled using the McKenzie heat flus model, with peak heat ffux density of 110 mW/m^2 reached during rifting (at 100Ma) and gradually dropping to a present day 53 mW/m^2. This choice of heat flux over the basin evolution resulted in a cement volume of just below 14% of available pore space. When syn-rift heat flux values between 65 and 110 mW/m^2 (Allen and Allen 2005) were used in the basin model, calculated cement volume remained effectively unchanged, presumably because the conditions for cementation had not been reached in the reservoir rocks. However, when the heat flux density was altered during the Miocene, the presumed time of quartz cementation onset, the calculated cement pore volume was significantly affected. Using a Miocene heat flux density of 35 mW/m^2 produces low cementation (< 8%) whereas a higher heat flus density of 65 mW/m^2 yielded relatively higher cementation (up to 17%). This is to be expected as effectively the time of onset of cementation is being changed.

Neither a variable peak heat flux nor a Miocene variation is justified geologically and basin models that incorporate these heat fluxes do not produce values that match present day measured temperature or vitrinite data. Nevertheless, these calculations are a good illustration of the significant impact of heat flux on quartz diagenesis where a change in heat flux value is justified.

Onset temperature for quartz cement: The onset temperature of quartz cementation has been reported to be between 70 and 135° C (Walderhaug, 1994, Walderhaug, 2000, Worden & Morad, 2000, Taylor et al., 2010). The bulk of the literature tends toward the lower end of this range for significant onset. Many of the models also have no lower cut-off temperature, but simply infer that reaction rates will be so low as to have no noticeable effect. For this study, we have taken the lower end of this range, i.e. 70° C, as the temperature for the onset of quartz precipitation in order to model the maximum likely adverse effect on potential reservoir properties. The Upper and Mid-Miocene has no evidence of quartz cementation, which is commensurate with its low formation temperature throughout its burial history. The Lower Miocene section shows a low volume of quartz cement (average of less than 5% of the pore space) in the study area, which can be attributed to the shallow burial depth of the sediments (800-1300m) with a temperature that has just entered the window for the onset of quartz cementation. However, the Oligocene section is buried at depths greater than 3800m and has therefore experienced temperatures exceeding 70° C for a longer time period. Our models show up to 14% of the pore space has suffered quartz cementation. We therefore suggest that our results, both observation and modelling, support the case for the onset of quartz cementation at the low end of the published temperature range.

Pressure: The Mid and Lower Miocene reservoirs do not develop overpressure in the 2D basin model but the Oligocene reservoirs do develop overpressure starting in the Mid-Miocene (14Ma) and continuing to increase up to the present day. Overpressure is typically expected to result in reduced cementation as compared with the hydrostatic equivalent. An in-depth investigation of the effect of overpressure development on cementation is beyond the scope of this study, but generally overpressure can be thought of as a fluid pressure state representative of a deeper location but at a lower temperature than would normally be associated with that deeper location. Here the model shows that the Oligocene reservoir becomes over-pressured at 14Ma, which is about 6Ma after the conditions for cementation

have been reached. If correct, earlier cementation will not have been affected by overpressure but later cementation may well have been retarded.

Hydrocarbons: Oil charge is another potential influence on cementation, though the effectiveness of petroleum in reducing cementation rate, or stopping it completely, is widely debated (Marchand et al. 2002; Wilkinson et al. 2004; Taylor et al., 2010). Hydrocarbon coating agents were observed during SEM analysis of the Mid-Miocene samples and dead oil was observed coating grains (Fig.8). Considering that early oil emplacement can halt or reduce quartz cement precipitation (Taylor et al., 2010), it is therefore possible that the presence of this oil seen only in the Mid-Miocene samples may have helped in preserving the porosity.

Comparative Oligocene Reservoirs

Here we briefly compare the potential Oligocene reservoirs of the Niger Delta that we have studied with two other Oligocene turbidite systems along the South Atlantic Margin: (1) the Lower Congo Basin, offshore Angola, and (2) the Campos Basin, offshore south-eastern Brazil. Of primary importance is the quality of the reservoirs and the corresponding key controlling factors.

The Lower Congo Basin is one of several different sub-basins developed along the West African passive margin, and is one of the most prolific, with major discoveries made within both Oligocene and Miocene turbidite systems of the Malembo Formation (Broucke et al., 2004). The most significant discoveries have been made in the Oligocene section, most notably the Girassol field, which has an estimated oil in place of 1550mmbbls and recoverable reserves placed at 725mmbbls trapped within Oligocene turbidite channel-levee complexes. The field is located within a water depth of 1350-1450m (Pelleau et al., 2002).

Whereas the Oligocene sediments of the Niger Delta slope system are found at depths greater than 3800m below sea level (up to 3000m sub-seafloor), the Oligocene reservoirs in Girassol field are located at a depth of 2400m below sea level (around 1000m sub seafloor). Clearly, the lower Congo Oligocene reservoirs have therefore undergone less burial and compaction. This is reflected in the wholly unconsolidated nature of the fine to very coarse sands, which exhibit excellent reservoir quality, having porosities of up to 40% and permeabilities greater than 5 Darcies. The Congo Basin reservoirs are also normally pressured with present day temperatures of 58–69° C (Dessus & Abreu, 2002, Pelleau et al., 2002, Delattre et al., 2004). The regional geology of the area does not suggest that the Malembo Formation has at any time been exposed to any physio-chemical conditions that would have led to the precipitation of any significant porosity-occluding diagenetic minerals, such as early quartz or calcite cements (Broucke et al., 2004, Gay et al., 2006).

Conjugate to the basins in West Africa is the Campos Basin of the Brazilian margin that lie beneath the coastal plain, continental shelf and slope along the western South Atlantic Ocean. The Campos Basin is the most prolific of the twelve east Brazilian offshore basins. (Bruhn et al., 2003). Turbidites constitute the main reservoir play in the Campos Basin, representing 37 different oilfields, including the Marlim Complex super giant field, which encompasses the Marlim Field itself and the surrounding fields of East Marlim, West Marlim and South Marlim (Souza et al., 1989, Bruhn et al., 2003). The total estimated oil in place for the Marlim Complex is about 13.9 billion barrels of oil, with the Marlim field itself accounting for over 57% of the

total volume of hydrocarbon (Souza et al., 1989). The principal reservoir of the Marlin field is the Oligocene Carapebus Member of the Campos Formation. The Marlim field was discovered by the first exploratory well drilled at a water depth of about 850m. The Oligocene reservoirs, located at a depth of about 2700m below sea level (i.e. < 2000m below seafloor), are known for three outstanding qualities: (1) predictability from seismic data, (2) good hydraulic connectivity, and (3) excellent petrophysical properties. Reservoir average porosities and permeabilities typically range between 27–30%, and 1000–2000mD respectively (Pinto et al., 2001).

The sand-rich reservoirs of the Marlim field comprise turbidite lobes, which accumulated in wide intra–slope depressions. The reservoir facies comprise mostly amalgamated graded beds of medium to very fine-grained sandstones that are poorly consolidated, poorly sorted and with a low volume of silt, clay and diagenetic minerals. The low degree of cementation in the Oligocene reservoirs is attributed to the following factors (Moraes, 1989; Soldan et al., 1995): (1) reservoir temperatures of about 80° C today and hence not long within the quartz-cementation window; (2) early oil emplacement that has inhibited cementation; (3) early carbonate cementation that persisted to depth and inhibited pressure dissolution; and (4) late-stage carbonate dissolution and creation of secondary porosity.

CONCLUSIONS

1. The potential Niger Delta Oligocene reservoir of the study area is interpreted to have been subjected to temperatures at or above 70° C from the Early Miocene to the present day. Our use of this temperature as the starting temperature for the onset of quartz precipitation is validated by the observation and modelling results presented.
2. Both petrological and petrophysical analysis of quartz in the Lower Miocene suggest an increase in quartz overgrowth volume with depth, indicating that the Oligocene sediments are likely to be cemented.
3. The possible volume of pore space occluded by cement in the Oligocene has been predicted to be (just) less than 14% of the available pore space.
4. Despite both modelled results and inferences suggesting the possibility of quartz cementation in the potential Oligocene reservoir, the quartz cement volume predicted from 2D simulation is not sufficient to prevent the Oligocene interval of the Agbada Formation from being a viable hydrocarbon reservoir.
5. The properties of comparable *Oligocene* reservoirs from the Lower Congo Basin and Campos Basin, are more similar to the reservoir properties of the *Miocene* turbidites of the Niger Delta that have been buried to a depth range of 2400–3000m, than those of the Oligocene system. It is very likely that one of the principal factors controlling reservoir quality is the depth of burial and the associated physiochemical conditions, since the best quality reservoirs are seen at depths of less than 3000m below sea level in all three basins.
6. Temperature-induced physical-chemical factors that favour quartz cementation are prevalent in sandstones buried deeper than 3000m within the Niger Delta deep-water system. The potential Oligocene reservoirs are currently located at depths > 3800m below sea level.
7. However, modelling carried out in this study suggest that reservoir properties of the Oligocene turbidite sands of the Niger Delta slope system are only slightly reduced

from those of the Miocene (up to 14% porosity occlusion). They therefore represent a very viable future exploration target.

8. We suggest that the integrated approach using petrological, petrophysical and basin modelling is an important and novel methodology with widespread application for more accurate prediction of sandstone reservoir quality in the subsurface.

ACKNOWLEDGEMENTS

REFERENCES

AJDUKIEWICZ, J. M. & LARESE, R. E. 2012. How clay grain coats inhibit quartz cement and preserve porosity in deeply buried sandstones: Observations and experiments. *AAPG bulletin,* 96**,** 2091-2119.

BILOTTI, F. & SHAW, J. H. 2005. Deep-water Niger Delta fold and thrust belt modeled as a critical-taper wedge: The influence of elevated basal fluid pressure on structural styles. *AAPG bulletin,* 89**,** 1475-1491.

BJØRKUM, P. A., OELKERS, E. H., NADEAU, P. H., WALDERHAUG, O. & MURPHY, W. M. 1998. Porosity prediction in quartzose sandstones as a function of time, temperature, depth, stylolite frequency, and hydrocarbon saturation. *AAPG Bulletin-American Association of Petroleum Geologists,* 82**,** 637.

BLOCH, S., LANDER, R. H. & BONNELL, L. 2002. Anomalously high porosity and permeability in deeply buried sandstone reservoirs: Origin and predictability. *AAPG bulletin,* 86**,** 301-328.

BRIGGS, S. E., CARTWRIGHT, J. & DAVIES, R. J. 2009. Crustal structure of the deepwater west Niger Delta passive margin from the interpretation of seismic reflection data. *Marine and Petroleum Geology,* 26**,** 936-950.

BROUCKE, O., TEMPLE, F., ROUBY, D., ROBIN, C., CALASSOU, S., NALPAS, T. & GUILLOCHEAU, F. 2004. The role of deformation processes on the geometry of mud-dominated turbiditic systems, Oligocene and Lower–Middle Miocene of the Lower Congo basin (West African Margin). *Marine and Petroleum Geology,* 21**,** 327-348.

BRUHN, C. H., GOMES, J. A. T., LUCCHESE JR, C. & JOHANN, P. R. Campos basin: reservoir characterization and management–Historical overview and future challenges. Offshore Technology Conference, Houston, Texas, USA, 2003. 5-8.

CORREDOR, F., SHAW, J. H. & BILOTTI, F. 2005. Structural styles in the deep-water fold and thrust belts of the Niger Delta. *AAPG bulletin,* 89**,** 753-780.

DELATTRE, E., AUTHIER, J. F., RODOT, F., PETIT, G. & ALFENORE, J. Review of sand control results and performance on a deep water development-A case study from the Girassol Field Angola. SPE Annual Technical Conference and Exhibition, 2004. Society of Petroleum Engineers.

DEPTUCK, M. E., SYLVESTER, Z., PIRMEZ, C. & O'BYRNE, C. 2007. Migration–aggradation history and 3-D seismic geomorphology of submarine channels in the Pleistocene Benin-major Canyon, western Niger Delta slope. *Marine and Petroleum Geology.*

DESSUS, J. L. & ABREU, J. 2002. Girassol: Drilling and Completion Experience gained through first 12 wells. *OTC,* 14168**,** 6-9.

DOUST, H. & OMATSOLA, E. 1990. Niger Delta. In:Edwards,J.D., Santogrossi, P.A (Eds), Divergent/Passive Margin Basins. *American Assoiciation of Petroleum Geologist,* 4**,** 239-248.

DOWEY, P.J., HODGSON, D.M. & WORDEN, R.H. 2012. Prerequisites, processes and prediction of chlorite grain coatings in petroleum reservoirs: A review of subsurface examples. *Marine & Petroleum Geology,* 32, 63-75.

EVANS, J., HOGG, A. J., HOPKINS, M. S. & HOWARTH, R. J. 1994. Quantification of quartz cements using combined SEM, CL, and image analysis. *Journal of Sedimentary Research,* 64.

FRENCH, M.W. & WORDEN, R.H. 2013. Orientation of microcrystalline quartz in the Fontainebleau Formation, Paris Basin and why it preserves porosity. *Sedimentary Geology,* 284-285, 149-158.

GAY, A., LOPEZ, M., COCHONAT, P., SÉRANNE, M., LEVACHÉ, D. & SERMONDADAZ, G. 2006. Isolated seafloor pockmarks linked to BSRs, fluid chimneys, polygonal faults and stacked Oligocene–Miocene turbiditic palaeochannels in the Lower Congo Basin. *Marine Geology,* 226**,** 25-40.

GIER, S., WORDEN, R. H., JOHNS, W. D. & KURZWEIL, H. 2008. Diagenesis and reservoir quality of Miocene sandstones in the Vienna Basin, Austria. *Marine and Petroleum Geology,* 25**,** 681-695.

HERMANRUD, C. 1993. Basin modelling techniques-an overview. *Basin modelling: advances and applications: Norwegian Petroleum Society (NPF) Special Publication,* 3**,** 1-34.

LANDER, R. H. & WALDERHAUG, O. 1999. Predicting porosity through simulating sandstone compaction and quartz cementation. *AAPG bulletin,* 83**,** 433-449.

MARCHAND, A. M., SMALLEY, P. C., HASZELDINE, R. S. & FALLICK, A. E. 2002. Note on the importance of hydrocarbon fill for reservoir quality prediction in sandstones. *AAPG bulletin,* 86**,** 1561-1572.

MCBRIDE, E. F. 1963. A classification of common sandstones. *Journal of Sedimentary Research,* 33.

MORAES, M. A. 1989. Diagenetic evolution of Cretaceous-Tertiary turbidite reservoirs, Campos Basin, Brazil. *AAPG Bulletin,* 73**,** 598-612.

NWACHUKWU, S. 1976. Approximate geothermal gradients in Niger Delta Sedimentary Basin. *AAPG Bulletin,* 60**,** 1073-1077.

PELLEAU, R., SERCEAU, A. & TOTALFINAELF 2002. The Girassol development: project challenges.

PETERS, K. E., MOLDOWAN, J. M., MCCAFFREY, M. A. & FAGO, F. J. 1996. Selective biodegradation of extended hopanes to 25-norhopanes in petroleum reservoirs. Insights from molecular mechanics. *Organic Geochemistry,* 24**,** 765-783.

PINTO, C., ANTONIO, C., GUEDES, S. S., BRUHN, C. H., GOMES, J. A. T. & NETTO, J. Marlim complex development: a reservoir engineering overview. SPE Latin American and Caribbean Petroleum Engineering Conference, 2001. Society of Petroleum Engineers.

REIJERS, T. 2011. Stratigraphy and sedimentology of the Niger Delta. *Geologos,* 17.

SAUGY, L. & EYER, J. A. 2003. Fifty years of exploration in the Niger Delta (West Africa).

SIEVER, R. 1983. Burial history and diagenetic reaction kinetics. *AAPG Bulletin,* 67**,** 684-691.

SNEIDER, R. M. 1990. Reservoir Description of Sandstones. *Sandstone Petroleum Reservoirs.* Springer.

SOLDAN, A., CERQUEIRA, J., FERREIRA, J., TRINDADE, L., SCARTON, J. & CORÁ, C. 1995. Giant Deep Water Oil Fields in Campos Basin, Brazil: A Geochemical Approach. *Revista Latino-Americana de Geoquimica Organica,* 1**,** 14-27.

SOMBRA, C. L. & CHANG, H. K. 1997. Burial history and porosity evolution of Brazilian Upper Jurassic to Tertiary sandstone reservoirs.

SOUZA, J., SCARTON, J., CANDIDO, A., CRUZ, C. & CORA, C. The Marlim and Albacora Fields: Geophysical Geological and Reservoir Aspects. Offshore Technology Conference, 1989. Offshore Technology Conference.

TALÇIN, M. N. 1991. Basin modeling and hydrocarbon exploration. *Journal of Petroleum Science and Engineering,* 5**,** 379-398.

TAYLOR, J. M. 1950. Pore-space reduction in sandstones. *AAPG Bulletin,* 34**,** 701-716.

TAYLOR, T. R., GILES, M. R., HATHON, L. A., DIGGS, T. N., BRAUNSDORF, N. R., BIRBIGLIA, G. V., KITTRIDGE, M. G., MACAULAY, C. I. & ESPEJO, I. S. 2010. Sandstone diagenesis and reservoir quality prediction: Models, myths, and reality. *AAPG bulletin,* 94**,** 1093-1132.

UNDERDOWN, R. & REDFERN, J. 2008. Petroleum generation and migration in the Ghadames Basin, north Africa: A two-dimensional basin-modeling study. *AAPG bulletin,* 92**,** 53-76.

WALDERHAUG, O. 1994. Precipitation rates for quartz cement in sandstones determined by fluid-inclusion microthermometry and temperature-history modeling. *Journal of Sedimentary Research,* 64**,** 324-333.

WALDERHAUG, O. 2000. Modeling quartz cementation and porosity in Middle Jurassic Brent Group sandstones of the Kvitebjørn field, northern North Sea. *AAPG bulletin,* 84**,** 1325-1339.

WEBER, K. 1971. Sedimentological aspects of oil fields in the Niger Delta. *Geologie en Mijnbouw,* 50**,** 559-576.

WELTE, D. & YALCIN, M. 1988. Basin modelling—a new comprehensive method in petroleum geology. *Organic Geochemistry,* 13**,** 141-151.

WHITEMAN, A. 1982. Nigeria: Its petroleum geology, resources and potential vol 1.

WILKINSON, M., STUART HASZELDINE, R., ELLAM, R. M. & FALLICK, A. 2004. Hydrocarbon filling history from diagenetic evidence: Brent Group, UK North Sea. *Marine and petroleum geology,* 21**,** 443-455.

WORDEN, R. & MORAD, S. 2000. Quartz cementation in oil field sandstones: a review of the key controversies. *Quartz cementation in sandstones,* 29**,** 1-20.

WYGRALA, B. 1988. Integrated computer-aided basin modeling applied to analysis of hydrocarbon generation history in a Northern Italian oil field. *Organic geochemistry,* 13**,** 187-197.

LIST OF FIGURES

Fig. 1. Regional location map showing the western Niger Delta and study area. Adapted from (Deptuck *et al.* 2007).

Fig. 2. Stratigraphy of the Niger Delta (after Corredor *et al.* 2005).

Fig. 3. Regional cross section showing the three structural provinces of the Niger Delta (modified from Corridor *et al.* 2005).

Fig. 4. Schematic illustration of ELAN. T represents the tool vector which in this case is the input log data (gamma ray, resistivity, neutron, density, and calculated porosity logs) and R is the response matrix which is a pre-defined value for the reading each tool would give for 100% of each formation component. R values were determined based on the known mineralogical responses to the physics of the different tools (Reeder *et al.*, 2013) as defined using the Schlumberger Techlog software package. V is the volume vector which is the volume of each formation components.

Fig. 5. Sedimentological log of core from well A1 across the Mid Miocene and Lower Miocene sections. Core photos represent typical examples of the lithologies described; Petrological samples taken from 'a' and 'b'.

Fig. 6. Photomicrographs in both plane polarised light and cross polars of Mid-Miocene (A, B) and Lower Miocene reservoirs (C,D), detrital quartz (QT-D), K-feldspar (Kf), polycrystalline (arrows).

Fig. 7. Upper Miocene polished block samples with no quartz cement seen from both BSE and CL plates (A and B), while overgrowths (indicated by amber arrow) are present in the Lower Miocene samples (C, D and E), detrital quartz (QT-D), quartz overgrowth (QT-OV), K-feldspar (Kf), heavy mineral (HM).

Fig. 8. BSE image of Upper Miocene samples showing quartz grains surrounded by oil.

Fig. 9. BSE images of Upper Miocene and Lower Miocene Sandstones. A and B images show authigenic kaolinite surrounded by oil. C shows pore filling kaolinite crystals [detrital quartz (QT-D), quartz overgrowth (QT-OV), oil, kaolinite (K)].

Fig. 10. Petrophysical data log showing modelled porosity calibrated to core porosity (track 6) and modelled permeability calibrated against core permeability (Track 7).

Fig. 11. Porosity-depth trend showing a reduction in porosity for several stacked reservoirs plotted against depth for 4 wells. Well A1, the deepest well highlighted in blue triangle with Oligocene porosity starting at 3500m.

Fig. 12. A) Modelled mineral volumes in track 8 (quartz=yellow, feldspar=pink, mica=black, kaolinite= cream with dash).Track 3;Gamma ray, track 4;resistivity;track 5; density, track 6; neutron and track 7; porosity, logs with suffix of ELAN represents back calculated logs: B) Cross plot of modelled quartz volume against depth

Fig. 13. Modelled thermal (A) and pressure (B) history. The pressure histories (B) are plots for both hydrostatic (line) and pore pressure (dash): (L=Lower Miocene, M= Middle Miocene and U= Upper Miocene).

Fig. 14. A) Interpreted regional 2D transect across the 3 structural provinces; B) Digitized 2D transect

Fig. 15. Overlay of predicted quartz cement on 2D transect.

Fig. 16. Fraction of pore space occluded by quartz cement plotted against depth: a 1D extract from the 2D model in Fig. 11. (Res=reservoir, P=Pliocene, UM= Upper Miocene, MM= Mid-Miocene, LM= Lower Miocene, UO= Upper Oligocene, LO= Lower Oligocene, E=Eocene).

Fig. 17. Modelled porosity (black line) versus depth calibrated against calculated porosity from well log (black cross). (Res=reservoir, P=Pliocene, UM= Upper Miocene, MM= Mid-Miocene, LM= Lower Miocene, UO= Upper Oligocene, LO= Lower Oligocene, E=Eocene).